
Faster Convergence of Riemannian Stochastic Gradient Descent with Increasing Batch Size

Kanata Oowada

*Department of Computer Science
Meiji University*

ce245014@meiji.ac.jp

Hideaki Iiduka

*Department of Computer Science
Meiji University*

iiduka@cs.meiji.ac.jp

Abstract

We have theoretically analyzed the use of Riemannian stochastic gradient descent (RSGD) and found that using an increasing batch size leads to faster RSGD convergence rate than using a constant batch size not only with a constant learning rate but also with a decaying learning rate, such as cosine annealing decay and polynomial decay. The convergence rate of RSGD improves from $O(\sqrt{T^{-1} + \text{const.}})$ with a constant batch size to $O(T^{-\frac{1}{2}})$ with an increasing batch size, where T denotes the number of iterations. Using principal component analysis and low-rank matrix completion tasks, we investigated, both theoretically and numerically, how increasing batch size affects computational time as measured by stochastic first-order oracle (SFO) complexity. Increasing batch size reduces the SFO complexity of RSGD. Furthermore, our numerical results demonstrated that increasing batch size offers the advantages of both small and large constant batch sizes.

1 Introduction

Stochastic gradient descent (SGD) Robbins & Monro (1951) is a basic algorithm, which is widely used in machine learning Liu et al. (2021); He et al. (2016); Krizhevsky et al. (2012). Riemannian stochastic gradient descent (RSGD) was proposed in Bonnabel (2013). Riemannian optimization Absil et al. (2008); Boumal (2023), which studies RSGD and its derivations, has been attracting attention for its use including many machine learning tasks. For example, it has been used in principal components analysis Breloy et al. (2021); Liu & Boumal (2020); Roy et al. (2018), low-rank matrix completion Vandereycken (2013); Nguyen et al. (2019); Boumal & Absil (2015); Kasai & Mishra (2016), convolutional neural networks Wang et al. (2020); Huang et al. (2017); Chen et al. (2017), graph neural networks Zhu et al. (2020); Chami et al. (2019); Liu et al. (2019), and has been used in applications of optimal transportation theory Lin et al. (2020b); Weber & Sra (2023).

It is well established that the performance of Euclidean SGD strongly depends on both the batch size (BS) and learning rate (LR) settings Goyal et al. (2017); Smith et al. (2018); Zhang et al. (2019); Lin et al. (2020a). In the context of Riemannian SGD, Ji et al. (2023); Bonnabel (2013); Kasai et al. (2019; 2018) addressed the use of a constant batch size and Sakai & Iiduka (2025); Han & Gao (2022) addressed the use of an adaptive BS (although the latter did not consider RSGD specifically). Additionally, Umeda & Iiduka (2024) found that increasing BS accelerated the convergence of Euclidean SGD. In parallel, various decaying LR strategies, including cosine annealing Loshchilov & Hutter (2017) and polynomial decay Chen et al. (2018), have been devised and their effectiveness has been demonstrated in the Euclidean case. Motivated by these findings, we have developed an approach that achieves a faster convergence rate for RSGD by using an increasing BS in combination with several types of a decaying LR schedules, including ones that have not yet been analyzed in the Riemannian context. Our numerical results demonstrate that an increasing BS leads to faster convergence in terms of both steps and computational time.

1.1 Previous Results and Our Contributions

Reference and Theorem	Batch Size	Learning Rate	Convergence Analysis
Bonnabel (2013)	–	s.a.r.	$\lim_{t \rightarrow \infty} \mathbb{E}[\text{grad}f(x_t)] = 0$ a.s.
Zhang & Sra (2016)	–	$\eta_t = O(\frac{1}{L_r + \sqrt{t}})$	$\mathbb{E}[f(\bar{x}_T) - f^*] = O(\frac{\sqrt{T}}{C+T})$
Tripuraneni et al. (2018)	Constant	$\eta_t = O(\frac{1}{t^\alpha})$	$\mathbb{E}\ \tilde{\Delta}_T\ = O(\frac{1}{\sqrt{T}})$
Hosseini & Sra (2020)	Constant	$\eta_t = O(\frac{1}{\sqrt{T}})$	$\ G_T\ = O(\frac{1}{\sqrt{T}})$
Durmus et al. (2021)	Constant	Constant	$\mathbb{E}[f(x_T) - f^*] = O(C_1^T + C_2)$
Sakai & Iiduka (2024)	Constant	$\eta_t = \frac{1}{\sqrt{t+1}}$	$\ G_T\ = O(\frac{\sqrt{\log T}}{\sqrt{T}})$
Sakai & Iiduka (2025)	Increasing	Constant	$\ G_T\ = O(\frac{1}{\sqrt{T}})$
Theorem 1	Constant	Constant and Decay	$\ G_T\ = O(\sqrt{\frac{1}{T} + C})$
Theorem 2	Increasing	Constant and Decay	$\ G_T\ = O(\frac{1}{\sqrt{T}})$
Theorem 3	Increasing	Warm-up	$\ G_T\ = O(\frac{1}{\sqrt{T-T_w}})$
Theorem 4	Constant	Warm-up	$\ G_T\ = O(\sqrt{\frac{1}{T-T_w} + C})$

Table 1: Comparison of RSGD convergence analyses, where $\alpha \in (\frac{1}{2}, 1)$, $C_1 \in (0, 1)$, C_2 and C are constants. For $\tilde{x}_t := R_{\tilde{x}_{t-1}}(\frac{1}{t}R_{\tilde{x}_{t-1}}^{-1}(x_t))$, $\tilde{\Delta}_t := R_{x^*}^{-1}(\tilde{x}_t)$. The usual stochastic approximation learning rate rule (s.a.r.) is defined as $\sum_{t=0}^{\infty} \eta_t = \infty$, $\sum_{t=0}^{\infty} \eta_t^2 < \infty$. T is the total number of iterations, and T_w is the number of warm-up iterations (see Section 3.3). $\min_{t \in \{0, \dots, T-1\}} \mathbb{E}[\|\text{grad}f(x_t)\|_{x_t}]$ is represented by $\|G_T\|$. ‘Decay’ includes diminishing LR.

Constraint: Bonnabel (2013); Zhang & Sra (2016); Durmus et al. (2021); Sakai & Iiduka (2024) considered Hadamard manifolds or their submanifolds. Tripuraneni et al. (2018) treated Riemannian manifolds that satisfy the condition required to ensure a unique geodesic connecting any two points, including Hadamard manifolds. Sakai & Iiduka (2025) addressed embedded submanifolds of Euclidean space. In contrast, we considered general Riemannian manifolds that encompass all of the above.

Learning rate: Bonnabel (2013) considered LRs satisfying $\sum_{t=0}^{\infty} \eta_t = \infty$, $\sum_{t=0}^{\infty} \eta_t^2 < \infty$, and Zhang & Sra (2016); Tripuraneni et al. (2018); Sakai & Iiduka (2024) considered diminishing LRs of the form $\eta_t = \frac{1}{t^\alpha}$. Hosseini & Sra (2020); Durmus et al. (2021) considered constant LRs. Sakai & Iiduka (2025) used both constant and diminishing LRs. We considered constant, diminishing, cosine annealing, and polynomial decay LRs, as well as these with warm-up.

Batch size: Since Bonnabel (2013) considered expected risk minimization using expectation instead of sample mean—as is customary in empirical risk minimization—the concept of batch size is not generally applicable in that context. Zhang & Sra (2016); Tripuraneni et al. (2018); Hosseini & Sra (2020); Durmus et al. (2021); Sakai & Iiduka (2024) considered a constant BS. Sakai & Iiduka (2025) and the present work considered an increasing BS. Furthermore, we numerically and theoretically compared using a constant BS and an increasing BS by using stochastic first-order oracle (SFO) complexity. Our contributions are as follows: (i) we theoretically showed that using an increasing BS yields a more favorable SFO rate of $O(\epsilon^{-2})$, whereas using a constant BS with the critical batch size yields a rate of $O(\epsilon^{-4})$; (ii) we numerically observed that increasing BS achieved both a better minimizer—in terms of attaining a smaller gradient norm—and a shorter computational time than using either a small or large constant BS (see Section 4.3 for more details).

Objective function: Bonnabel (2013) considered three times continuously differentiable, with both the gradient and Hessian uniformly bounded. Tripuraneni et al. (2018) treated functions that are twice continuously differentiable, subject to additional conditions on the Hessian. Other studies considered only once continuously differentiability. Zhang & Sra (2016) addressed convex and smooth functions, while Durmus et al. (2021) considered strongly convex and smooth functions. Hosseini & Sra (2020); Sakai & Iiduka (2024; 2025) treated more general classes of functions, specifically nonconvex functions with bounded gradients. We treated nonconvex functions without bounded gradients.

Convergence rate: A comparison of the previous and current RSGD convergence analyses is presented in Table 1.1; here we outline the key results. Tripuraneni et al. (2018) obtained a convergence rate of $O(\frac{1}{\sqrt{T}})$ (with a criterion other than the gradient norm) using a learning rate of $\eta = O(\frac{1}{\sqrt{T}})$; however, this rate decays to zero as $T \rightarrow \infty$, making it unsuitable for practical use. Durmus et al. (2021) attained exponential convergence under strong convexity and smoothness assumptions. Sakai & Iiduka (2025) attained a rate of $O(\frac{1}{\sqrt{T}})$ for several adaptive methods, including RSGD. In contrast, our work differs from Sakai & Iiduka (2025) in four key aspects : (i) we provide both theoretical and numerical evidence—based on SFO complexity—that using an increasing batch size leads to better performance than using a fixed batch size; (ii) in addition to a constant LR and diminishing LR, we addressed cosine annealing, polynomial decay, and warm-up LR; (iii) Sakai & Iiduka (2024) focused on embedded submanifolds of Euclidean space unlike us; (iv) we do not assume bounded gradient norms, thus expanding the range of applicable scenarios.

Summary:

- We developed a convergence analysis of RSGD incorporating increasing BS, cosine annealing LR, and polynomial decay LR, under assumptions that are more general than those used in prior work. Our analysis demonstrates that using an increasing BS improves the convergence rate of RSGD from $O(\sqrt{\frac{1}{T} + C})$ to $O(\frac{1}{\sqrt{T}})$.
- We numerically and theoretically demonstrated—using PCA and low-rank matrix completion (LRMC) tasks—the advantage of increasing BS for computational time via SFO complexity. Specifically, we observed that increasing BS yields a better minimizer (compared with a small constant BS) in term of achieving a small gradient norm and a shorter computational time (compared with a large constant BS). These findings are consistent with our theoretical analysis, which shows that increasing BS improves the SFO rate for reaching $\|G_T\|^2 \leq \epsilon^2$ from $O(\epsilon^{-4})$ (under constant BS with critical batch size) to $O(\epsilon^{-2})$ (under increasing BS in the experimental setting).

2 Preliminaries

Let \mathcal{M} be a Riemannian manifold. $T\mathcal{M}$ denotes the tangent bundle of \mathcal{M} . For all $x \in \mathcal{M}$, the inner product of \mathcal{M} is represented $\langle \cdot, \cdot \rangle_x$ on $T_x\mathcal{M}$ and induce the norm $\|\cdot\|_x$. For a smooth map $f: \mathcal{M} \rightarrow \mathbb{R}$, we can define gradient $\text{grad}f$ as a unique vector field that satisfies $\forall v \in T_x\mathcal{M}: Df(x)[v] = \langle \text{grad}f(x), v \rangle_x$. Although, in Euclidean space, iterative methods are updated by addition, Riemannian manifold does not equipped with addition generally. There is an alternative of updating procedure as follows.

Definition 1 (Retraction). *Let 0_x be a zero element of $T_x\mathcal{M}$. When a map $R: T\mathcal{M} \ni (x, v) \mapsto R_x(v) \in \mathcal{M}$ satisfies the following conditions, R is referred to as a retraction on \mathcal{M} .*

1. $R_x(0_x) = x$,
2. With the canonical identification $T_{0_x}T_x\mathcal{M} \simeq T_x\mathcal{M}$, $DR_x(0_x) = \text{id}_{T_x\mathcal{M}}$ for all $x \in \mathcal{M}$,

where $\text{id}_{T_x\mathcal{M}}: T_x\mathcal{M} \rightarrow T_x\mathcal{M}$ is the identity mapping.

Iterative methods on Riemannian manifold are defined by $x_{t+1} = R_{x_t}(\eta_t d_t)$ generally. Exponential maps are often used as retractions. The following assumption plays a central role in Lemma 1.

Assumption 1 (Retraction Smoothness). *Let $f: \mathcal{M} \rightarrow \mathbb{R}$ be a smooth map. Then there exists $L_r > 0$ such that, for all $x \in \mathcal{M}$ and all $v \in T_x\mathcal{M}$,*

$$f(R_x(v)) \leq f(x) + \langle \text{grad}f(x), v \rangle_x + \frac{L_r}{2} \|v\|_x^2.$$

In the Euclidean space setting, L -smoothness implies a property similar to retraction smoothness. The property corresponding to L -smoothness in Euclidean space is defined for $f: \mathcal{M} \rightarrow \mathbb{R}$ as

$$\exists L > 0, \forall x, y \in \mathcal{M}: \|\text{grad}f(x) - \Gamma_y^x \text{grad}f(y)\|_x \leq L_r d(x, y),$$

where Γ is the parallel transport from $T_y\mathcal{M}$ to $T_x\mathcal{M}$, and $d(\cdot, \cdot)$ is the Riemannian distance. This is a sufficient condition for Assumption 1 with $R := \text{Exp}$ (see Boumal (2023, Corollary 10.54)). This case is frequently used (e.g., Zhang & Sra (2016); Criscitiello & Boumal (2023); Kim & Yang (2022); Liu et al. (2017)). Other sufficient conditions for Assumption 1 were identified by Kasai et al. (2018, Lemma 3.5) or Sakai & Iiduka (2025, Proposition 3.2). Now, we consider the empirical risk minimization problem such that

$$\underset{x \in \mathcal{M}}{\text{minimize}} \quad f(x) := \frac{1}{N} \sum_{j=1}^N f_j(x),$$

where every $f_j: \mathcal{M} \rightarrow \mathbb{R}$ is smooth and lower bounded. Therefore, f satisfies the same conditions. This assumption is often made for both Euclidean space and Riemannian space. The lower boundedness of f is essential for analyses using optimization theory since unbounded f may not have optimizers. We denote a minimizer of f as x^* ($f^* := f(x^*)$) and denote N is the size of a dataset. In many machine learning tasks, the dimension of model parameters x or the size of dataset N is large. Hence, we use the following mini-batch gradient to efficiently approximate the gradient of f .

$$\text{grad}f_B(x) := \frac{1}{b} \sum_{j=1}^b \text{grad}f_{\xi_j}(x),$$

where B represents a minibatch with size b , and $(\xi_j)_j$ is a $\{1, \dots, N\}$ -valued i.i.d. copy. Namely, the gradient of $f_B(x) = \frac{1}{b} \sum_{j=1}^b f_{\xi_j}(x)$ is used instead of $\text{grad}f(x)$. The following assumption is reasonable given this situation.

Assumption 2 (Bounded Variance Estimator). *The stochastic gradient given by a distribution Π is an unbiased estimator and has a bounded variance:*

1. $\forall x \in \mathcal{M}: \mathbb{E}_{\xi \sim \Pi} [\text{grad}f_{\xi}(x)] = \text{grad}f(x)$,
2. $\exists \sigma > 0, \forall x \in \mathcal{M}: \mathbb{V}_{\xi \sim \Pi}(\text{grad}f_{\xi}(x)) \leq \sigma^2$.

Remark 1. *Note that, from 1, $\mathbb{V}_{\xi \sim \Pi}(\text{grad}f_{\xi}(x)) = \mathbb{E}_{\xi \sim \Pi} [\|\text{grad}f_{\xi}(x) - \text{grad}f(x)\|_x^2]$ holds.*

For example, if f being lower bounded satisfies Assumption 1 and one takes the uniform distribution as Π , then Assumption 2 holds. RSGD is defined as

$$x_{t+1} = R_{x_t}(-\eta_t \text{grad}f_{B_t}(x_t)).$$

We suppose that the sequence $(x_t)_t$ generated by RSGD is independent of random variables $(\xi_{j,t})_{j,t}$ for the minibatch gradient. Note that the BS $(b_t)_t$ is variable at each step.

3 Convergence Analysis

First, we prepare some lemmas for the convergence analysis of RSGD.

Lemma 1 (Descent Lemma). *Let $(x_t)_t$ be a sequence generated by RSGD and $(\eta_t)_t$ be a positive valued sequence. Then, under Assumptions 1 and 2, we obtain*

$$\mathbb{E}[f(x_{t+1})] \leq \mathbb{E}[f(x_t)] + \frac{L_r \sigma^2 \eta_t^2}{2b_t} - \eta_t \left(1 - \frac{L_r \eta_t}{2}\right) \mathbb{E}[\|\text{grad}f(x_t)\|_{x_t}^2].$$

Lemma 1 implies Lemma 2 which plays a central role over the following convergence analyses. The proofs of both lemmas are given in Appendices C.1 and C.2.

Lemma 2 (Underlying Analysis). *Let $(x_t)_t$ be a sequence generated by RSGD and $\eta_{\max} > 0$. We consider a positive valued sequence $(\eta_t)_t$ such that $\eta_t \in [0, \eta_{\max}] \subset [0, \frac{2}{L_r}]$. Then, under Assumptions 1 and 2, we obtain*

$$\min_{t \in \{0, \dots, T-1\}} \mathbb{E}[\|\text{grad}f(x_t)\|_{x_t}^2] \leq \frac{2(f(x_0) - f^*)}{2 - L_r \eta_{\max}} \frac{1}{\sum_{t=0}^{T-1} \eta_t} + \frac{L_r \sigma^2}{2 - L_r \eta_{\max}} \frac{\sum_{t=0}^{T-1} \eta_t^2 b_t^{-1}}{\sum_{t=0}^{T-1} \eta_t}.$$

3.1 Case (i): Constant BS; Constant or Decaying LR

In this case, we consider a BS $(b_t)_t$ and a LR $(\eta_t)_t$ such that $b_t = b$ and $\eta_{t+1} \leq \eta_t$. In particular, we set the following examples with constant or decaying LR.

$$\text{Constant LR: } \eta_t = \eta_{\max}, \quad (1)$$

$$\text{Diminishing LR: } \eta_t = \frac{\eta_{\max}}{\sqrt{t+1}}, \quad (2)$$

$$\text{Cosine Annealing LR: } \eta_t := \eta_{\min} + \frac{\eta_{\max} - \eta_{\min}}{2} \left(1 + \cos \frac{t}{T} \pi \right), \quad (3)$$

$$\text{Polynomial Decay LR: } \eta_t := \eta_{\min} + (\eta_{\max} - \eta_{\min}) \left(1 - \frac{t}{T} \right)^p, \quad (4)$$

where η_{\max} and η_{\min} are positive values satisfying $0 \leq \eta_{\min} \leq \eta_{\max} < \frac{2}{L_r}$. Note that η_{\max} (resp. η_{\min}) becomes the maximum (resp. minimum) of η_t ; namely, $\eta_t \in [\eta_{\min}, \eta_{\max}] \subset [0, \frac{2}{L_r}]$.

Theorem 1. *We consider LR equation 1, equation 2, equation 3, and equation 4 and a constant BS $b_t = b > 0$ under the assumptions of Lemma 2. Then, we obtain*

- *Diminishing LR equation 2*

$$\min_{t \in \{0, \dots, T-1\}} \mathbb{E}[\|\text{grad}f(x_t)\|_{x_t}^2] \leq \frac{Q_1 + Q_2 \sigma^2 b^{-1} \log T}{\sqrt{T}},$$

- *Otherwise equation 1, equation 3, equation 4*

$$\min_{t \in \{0, \dots, T-1\}} \mathbb{E}[\|\text{grad}f(x_t)\|_{x_t}^2] \leq \frac{\tilde{Q}_1}{T} + \frac{\tilde{Q}_2 \sigma^2}{b},$$

where Q_1, Q_2, \tilde{Q}_1 , and \tilde{Q}_2 are constants which do not depend on T .

Therefore, a diminishing LR equation 2 has $\|G_T\| = O\left(\frac{\sqrt{\log T}}{\sqrt{T}}\right)$, whereas equation 1, equation 3, and equation 4 have $\|G_T\| = O\left(\sqrt{\frac{1}{T} + \frac{\sigma^2}{b}}\right)$. The proof is in Appendix C.3.

3.2 Case (ii): Increasing BS; Constant or Decaying LR

In this case, we consider a BS $(b_t)_t$ and a LR $(\eta_t)_t$ such that $b_t \leq b_{t+1}$ and $\eta_{t+1} \leq \eta_t$. We use the four examples with constant or decaying LR *equation 1, \dots , equation 4* in **Case (i)** (Section 3.1) and a BS that increases every K ($\in \mathbb{N}$) steps. We let T be the total number of iterations and define $M := \lfloor \frac{T}{K} \rfloor$ to represent the number of times the BS is increased. The BS, which takes the form of $\gamma^m b_0$ or $(am + b_0)^p$ every K steps, serves as an example of an increasing BS. We can formalize the resulting BSs: for every $m \in \{0, \dots, M-1\}, t \in S_m := [mK, (m+1)K) \cap \mathbb{N}$ ($S_0 := [0, K)$)

$$\text{Exponential Growth BS: } b_t := b_0 \gamma^{m \lceil \frac{t}{(m+1)K} \rceil}, \quad (5)$$

$$\text{Polynomial Growth BS: } b_t := \left(am \left\lceil \frac{t}{(m+1)K} \right\rceil + b_0 \right)^c, \quad (6)$$

where $\gamma, c > 1$, and $a > 0$. One can easily check this. (For example, $\frac{m}{m+1} \leq \left\lceil \frac{t}{(m+1)K} \right\rceil < 1$ ($\forall t \in S_m$) holds.)

Theorem 2. *We consider BSs equation 5 and equation 6 and LR equation 1, equation 2, equation 3, and equation 4 under the assumptions of Lemma 2. Then, the following holds for both constant and increasing BSs.*

- *Diminishing LR equation 2*

$$\min_{t \in \{0, \dots, T-1\}} \mathbb{E}[\|\text{grad}f(x_t)\|_{x_t}^2] \leq \frac{Q_1 + Q_2 \sigma^2 b_0^{-1}}{\sqrt{T}},$$

- *Otherwise equation 1, equation 3, equation 4*

$$\min_{t \in \{0, \dots, T-1\}} \mathbb{E}[\|\text{grad}f(x_t)\|_{x_t}^2] \leq \frac{\tilde{Q}_1 + \tilde{Q}_2 \sigma^2 b_0^{-1}}{T},$$

where Q_1, Q_2, \tilde{Q}_1 , and \tilde{Q}_2 are constants which do not depend on T .

Therefore, the diminishing LR equation 2 has $\|G_T\| = O(\frac{1}{\sqrt{T}})$, and the other LRs equation 1, equation 3, and equation 4 have $\|G_T\| = O(\frac{1}{\sqrt{T}})$. The proof is in Appendix C.4.

3.3 Case (iii): Increasing BS; Warm-up Decaying LR

In this case, we consider a BS $(b_t)_t$ and a LR $(\eta_t)_t$ such that $b_t \leq b_{t+1}$ and $\eta_t \leq \eta_{t+1}$ ($t \leq T_w - 1$), $\eta_{t+1} \leq \eta_t$ ($t \geq T_w$). As examples of an increasing warm-up LR, we use an exponentially increasing LR and a polynomially increasing LR, both increasing every K' steps. We set K , which was defined in **Case (ii)** (Section 3.2), as lK' , where $l \in \mathbb{N}$ (thus, $K > K'$). Namely, we consider a setting in which the BS is increased every l times the LR is increased. To formulate examples of an increasing LR, we define $M' := \lfloor \frac{T}{K'} \rfloor$ and formalize the LR: for every $m \in \{0, \dots, M' - 1\}$, $t \in S'_m := [mK', (m+1)K') \cap \mathbb{N}$ ($S'_0 := [0, K')$),

$$\text{Exponential Growth LR: } \eta_t := \eta_0 \delta^m \left\lceil \frac{t}{(m+1)K'} \right\rceil, \quad (7)$$

$$\text{Polynomial Growth LR: } \eta_t := \left(sm \left\lceil \frac{t}{(m+1)K'} \right\rceil + \eta_0 \right)^q, \quad (8)$$

where $s > 0$ and $q > 1$. Furthermore, we choose $\gamma, \delta > 1$, and $l \in \mathbb{N}$ such that $\delta^{2l} < \gamma$ holds. Additionally, we set $l_w \in \mathbb{N}$ such that $T \geq T_w := l_w K' \geq lK'$. The examples of an increasing BS used in this case are an [exponential growth BS] equation 5 and a polynomial growth BS equation 6. As examples of a warm-up LR, we consider LRs that are increased using exponential growth LR equation 7 and polynomial growth LR equation 8 corresponding to the exponential and polynomial growth BSs for the first T_w steps and then decreased using a constant LR equation 1, a diminishing LR equation 2, a cosine annealing LR equation 3, and a polynomial decay LR equation 4 for the remaining $T - T_w$ steps. Note that $\eta_{\max} := \eta_{T_w - 1}$.

Theorem 3. *We consider BSs equation 5 and equation 6 and warm-up LRs equation 7 and equation 8 with decay parts equation 1, equation 2, equation 3, and equation 4 under the assumptions of Lemma 2. Then, the following holds for both constant and increasing BSs.*

- *Decay part: Diminishing equation 2*

$$\min_{t \in \{T_w, \dots, T-1\}} \mathbb{E}[\|\text{grad}f(x_t)\|_{x_t}^2] \leq \frac{Q_1 + Q_2 \sigma^2 b_0^{-1}}{\sqrt{T+1} - \sqrt{T_w+1}},$$

- *Decay part: Otherwise equation 1, equation 3, equation 4*

$$\min_{t \in \{T_w, \dots, T-1\}} \mathbb{E}[\|\text{grad}f(x_t)\|_{x_t}^2] \leq \frac{\tilde{Q}_1 + \tilde{Q}_2 \sigma^2 b_0^{-1}}{T - T_w},$$

where Q_1, Q_2, \tilde{Q}_1 , and \tilde{Q}_2 are constants which do not depend on T .

Therefore, the diminishing LR equation 2 has $\|G_T\| = O(\frac{1}{\sqrt{\sqrt{T+1} - \sqrt{T_w+1}}})$, and the other LRs equation 1, equation 3, and equation 4 have $\|G_T\| = O(\frac{1}{\sqrt{T-T_w}})$. The proof is in Appendix C.5.

3.4 Case (iv): Constant BS; Warm-up Decaying LR

In this case, we consider a BS $(b_t)_t$ and a LR $(\eta_t)_t$ such that $b_t = b$ and $\eta_t \leq \eta_{t+1}$ ($t \leq T_w - 1$), $\eta_{t+1} \leq \eta_t$ ($t \geq T_w$). As examples of a warm-up LR, we use an exponential growth LR equation 7 and a polynomial growth LR equation 8 for the first T_w steps and then a constant LR equation 1, diminishing LR equation 2, cosine annealing LR equation 3, or polynomial decay LR equation 4 for the remaining $T - T_w$ steps. The other conditions are the same as in **Case (iii)** (Section 3.3).

Theorem 4. *We consider a constant BS $b_t = b > 0$ and warm-up LRs equation 7 and equation 8 with decay parts equation 1, equation 2, equation 3, or equation 4 under the assumptions of Lemma 2. Then, we obtain*

- *Decay part: Diminishing equation 2*

$$\min_{t \in \{T_w, \dots, T-1\}} \mathbb{E}[\|\text{grad}f(x_t)\|_{x_t}^2] \leq \left(Q_1 + \frac{Q_2\sigma^2}{b} \log \frac{T}{T_w}\right) \frac{1}{\sqrt{T+1} - \sqrt{T_w+1}},$$

- *Decay part: Otherwise equation 1, equation 3, equation 4*

$$\min_{t \in \{T_w, \dots, T-1\}} \mathbb{E}[\|\text{grad}f(x_t)\|_{x_t}^2] \leq \frac{\tilde{Q}_1}{T - T_w} + \frac{\tilde{Q}_2\sigma^2}{b},$$

where Q_1, Q_2, \tilde{Q}_1 , and \tilde{Q}_2 are constants which do not depend on T .

Therefore, the diminishing LR equation 2 has $\|G_T\| = O\left(\sqrt{\frac{\log T - \log T_w}{\sqrt{T+1} - \sqrt{T_w+1}}}\right)$, and the other LR equation 1, equation 3, and equation 4 have $\|G_T\| = O\left(\sqrt{\frac{1}{T-T_w} + \frac{\sigma^2}{b}}\right)$. The proof is in Appendix C.6.

4 Numerical Experiment

We experimentally evaluated the performance of RSGD for the two types of BSs and various types of LR introduced in Section 3. They were run on an iMac (Intel Core i5, 2017) running the macOS Ventura operating system (ver. 13.7.1). The algorithms were written in Python (3.12.7) using the NumPy (1.26.0) and Matplotlib (3.9.1) packages. The Python codes are available at https://anonymous.4open.science/r/faster_rsgd-CE24. We set $p = 2.0$ in equation 4 and $\eta_{\min} := 0$. In **Cases (i) and (ii)**, we used an initial LR η_{\max} selected from $\{0.5, 0.1, 0.05, 0.01, 0.005\}$. In **Case (ii)**, we set $K = 1000, \gamma = 3.0$ and $a = c = 2.0$. The plots of the objective function values corresponding to this section are in Appendix B and Appendix D. The results for **Cases (iii) and (iv)** are given in Appendix E.

4.1 Principal Component Analysis

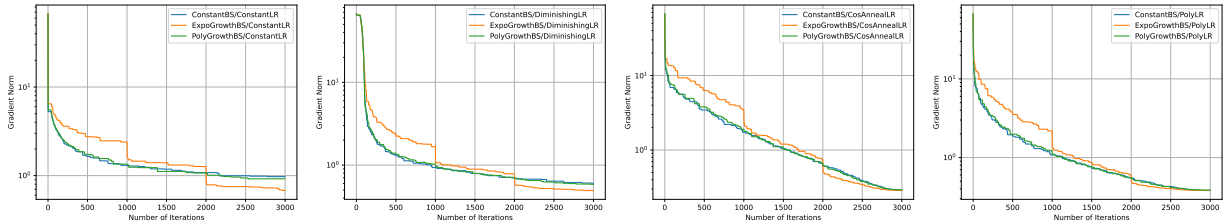


Figure 1: Norm of the gradient of the objective function against number of iterations for LR equation 1, equation 2, equation 3, and equation 4 on COIL100 dataset.

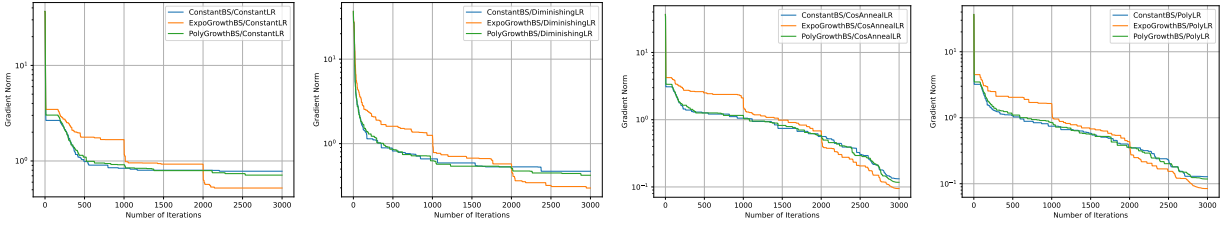


Figure 2: Norm of the gradient of the objective function against number of iterations for LR equation 1, equation 2, equation 3, and equation 4 on MNIST dataset.

We can formulate the principal component analysis (PCA) problem as an optimization problem on the Stiefel manifold Kasai et al. (2019); for a given dataset $\{x_j\}_{j=1,\dots,N} \subset \mathbb{R}^n$ and $r (\leq n)$,

$$\begin{aligned} & \text{minimize} && f(U) := \frac{1}{N} \sum_{j=1}^N \|x_j - UU^T x_j\|^2, \\ & \text{subject to} && U \in \text{St}(r, n) := \{U \in \mathbb{R}^{r \times n} \mid U^T U = I_n\}. \end{aligned}$$

We set $r = 10$ and used the COIL100 Nene et al. (1996) and MNIST LeCun et al. (1998) datasets. The Columbia Object Image Library (COIL100) dataset contains 7200 color camera images of 100 objects (72 poses per object) taken from different angles. We resized the images to 32×32 pixels and transformed each one into a $1024 (= 32^2)$ dimensional vector. Hence, we set $(N, n, r) = (7200, 1024, 10)$. The MNIST dataset contains 60,000 28×28 -pixel gray-scale images of handwritten numbers 0 to 9. We transformed each image into a $784 (= 28^2)$ dimensional vector and normalized each pixel to the range $[0, 1]$. Hence, we set $(N, n, r) = (60000, 784, 10)$. Furthermore, we used a constant BS with $b_t := 2^{10}$, an exponential growth BS with an initial value $b_0 := 3^5$, and a polynomial growth BS with an initial value $b_0 := 30$.

4.2 Low-rank Matrix Completion

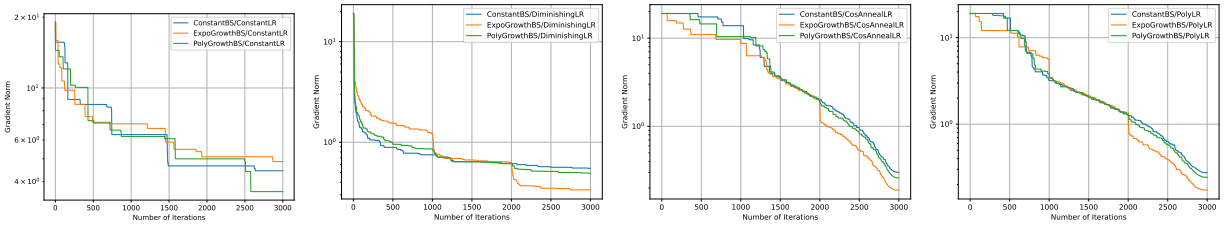


Figure 3: Norm of the gradient of the objective function against number of iterations for LR equation 1, equation 2, equation 3, and equation 4 on MovieLens-1M dataset.

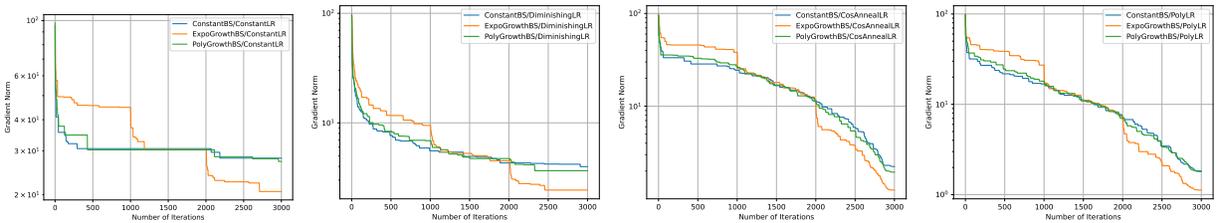


Figure 4: Norm of the gradient of the objective function against number of iterations for LR equation 1, equation 2, equation 3, and equation 4 on Jester dataset.

The LRMC problem involves completing an incomplete matrix $Z = (z_1, \dots, z_N) \in \mathbb{R}^{n \times N}$; Ω denotes a set of indices for which we know the entries in Z . For $a \in \mathbb{R}^n$, we define $P_{\Omega_i}(a)$ such that the j -th element is

	COIL100 (PCA)	MNIST (PCA)	MovieLens-1M (LRMC)	Jester (LRMC)
Large BS	1411.37	2697.24	4482.41	5432.54
Full BS	1488.34	2719.66	12947.91	6816.28
Increasing BS	468.53	745.13	1133.92	1695.85

Table 2: Computational time [sec] (CPU time) for large, full, and increasing batch size.

a_j if $(i, j) \in \Omega$ and 0 otherwise. For $U \in \mathbb{R}^{n \times r}$, $z \in \mathbb{R}^n$, $q_j(U, z) := \operatorname{argmin}_{a \in \mathbb{R}^r} \|P_{\Omega_j}(Ua - z)\|$. We can now formulate the LRMC problem as the following optimization problem on the Grassmann manifold Boumal & Absil (2015);

$$\begin{aligned} \text{minimize} \quad & f(U) := \frac{1}{N} \sum_{j=1}^N \|P_{\Omega_j}(Uq_j(U, z_j) - z_j)\|^2, \\ \text{subject to} \quad & U \in \operatorname{Gr}(r, n) := \operatorname{St}(r, n)/O(r), \end{aligned}$$

where $O(r)$ is the r -dimensional orthogonal group. We set $r = 10$ and used the MovieLens-1M Harper & Konstan (2016) and Jester datasets Goldberg et al. (2001). The MovieLens-1M dataset contains 1,000,209 ratings given by 6040 users on 3952 movies. Every rating lies in $[0, 5]$. We normalized each rating to the range $[0, 1]$. Hence, we set $(N, n, r) = (3952, 6040, 10)$. The Jester dataset contains ratings of 100 jokes from 24,983 users. Every rating lies in the range $[-10, 10]$. Hence, we set $(N, n, r) = (24983, 100, 10)$. Furthermore, we used a constant BS with $b_t := 2^8$, an exponential growth BS with an initial value $b_0 := 3^4$, and an polynomial growth BS with an initial value $b_0 := 14$.

The performance in terms of the gradient norm of the objective function against the number of iterations for LR equation 1, equation 2, equation 3, and equation 4 on the COIL100, MNIST, MovieLens-1M, and Jester datasets are plotted in Figures 1, 2, 3, and 4, respectively. The performance in terms of achieving a small gradient norm was better with an increasing BS than with a constant BS. Even in increasing BSs, an exponential growth BS showed better performance than a polynomial BS. Since the magnitude of increase in an exponential BS is $O(\gamma^m)$ and it of a polynomial BS is $O(m)$, this numerical results demonstrated that a larger increase in BS leads to better performance. Although the differences in the objective function values are small (one possible reason for this is that the objective function may be flat around the optimal solution), the performance of an increasing BS was equal to or better than a constant BS.

4.3 Comparison of Computational Time between Constant BS and Increasing BS via SFO Complexity

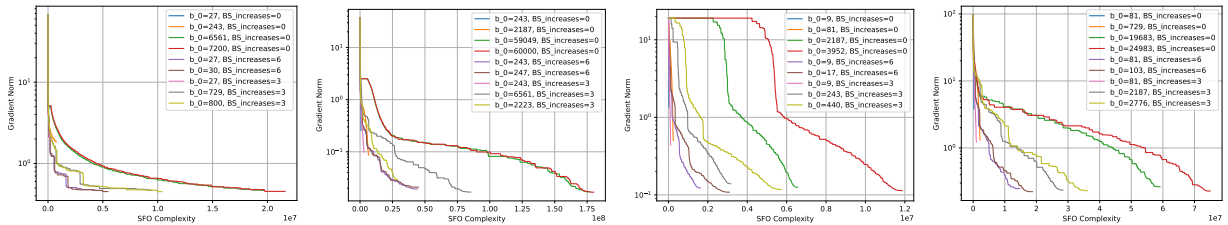


Figure 5: Norm of objective function gradient versus SFO complexity. Datasets used were COIL100 (PCA), MNIST (PCA), MovieLens-1M (LRMC), and Jester (LRMC) in order from left to right. A cosine annealing LR was used except COIL100, for which a constant LR was used. For ‘BS-increases= 0,’ a constant BS $b = b_0$ was used. For ‘BS-increases= 3’ and ‘BS-increases= 6,’ the BS was increased 3 and 6 times, respectively, in accordance with the exponential-growth BS schedule.

What are the differences among using a large constant BS, a small constant BS, and an increasing BS? We numerically investigate this question on the basis of SFO complexity, which is defined by the number of stochastic gradient evaluations executed over T iterations Agarwal & Bottou (2015); Shallue et al. (2019); Sato & Iiduka (2023). For a constant BS b , it is represented by bT . SFO complexity for other BSs can be calculated numerically, serving as a proxy for computational time. Figure 5 plots the gradient norm of

the objective function against SFO complexity for PCA and LRMC. Each curve corresponds to RSGD for 3000 steps under one of the following settings: constant BS, BS tripled every 1000 steps (three increases in total), or BS tripled every 500 steps (six increases in total). These settings follow the update formula for constant or exponential growth BS. Additional experimental details are given in the caption of Figure 5. As shown in the figure, increasing BS combines the advantages of both small and large BSs, namely shorter computational time and convergence to a solution with a smaller final gradient norm).

As shown in Figure 5, although both full and large constant BSs lead to minimizers achieving a small gradient norm, they require more SFO complexity. In contrast, while small constant BSs require fewer SFO complexity, they do not lead to minimizers achieving a small gradient norm. Increasing BSs with many increments and a small initial batch size lead to minimizers achieving a small gradient norm with relatively few SFO complexity. As shown in Table 2, the computational time (CPU time) of increasing BS is shorter than that of both large and full constant BSs. Between small and large constant BSs, there is a trade-off between convergence to a solution with a smaller final gradient norm and a shorter computational time. Our results demonstrate that an increasing BS balances this trade-off effectively.

Why is increasing BS better? Our theoretical analyses provide an answer to this question. From Theorem 1, the SFO complexity of a constant BS with the critical BS for achieving $\|G_T\|^2 \leq \epsilon^2$ is $O(\epsilon^{-4})$. From the same theorem, the SFO complexity of an exponential growth BS for achieving $\|G_T\|^2 \leq \epsilon^2$ is $O(\gamma^{\epsilon^{-2}})$, where $\gamma := 3$ in this experiment. Although $O(\gamma^{\epsilon^{-2}})$ is inferior to $O(\epsilon^{-4})$ in our strict theoretical setting—fixed K (number of steps for each BS) and dynamic M (number of BS increases)—the assumptions in this experiment differed. Specifically, K depended on the value assigned to M , and our analysis can be applied to this experimental setting. Under these conditions, the SFO complexity of an exponential growth BS for achieving $\|G_T\|^2 \leq \epsilon^2$ is $O(\epsilon^{-2})$, which is superior to $O(\epsilon^{-4})$. This provides our theoretical justification: increasing BS achieves lower SFO complexity than constant BS. Moreover, even among increasing BS settings, performance was better for $M = 6$ than for $M = 3$; i.e., performance improves with the number of BS increments. From Theorem 2, we have $\|G_T\| = O(\sqrt{\frac{1}{T} + \frac{1}{M}})$, indicating that a larger M leads to a smaller gradient norm and explains the observed phenomenon. The relevant derivations are provided in Appendix A.

Remark 2. *Under the rigorous conditions of our theory, $M \rightarrow \infty$ implies that $T = MK + \text{const.} \rightarrow \infty$ with K fixed. In contrast, the conditions of our experiment do not permit an increase in BS to achieve $T \rightarrow \infty$ because it requires $K \rightarrow \infty$ for T to diverge with a fixed M , which means that the number of steps for the initial batch size is infinite. However, as is done in many experimental setups, including ours, T is predetermined as a finite value before conducting the experiment. This setting is equivalent to using the number of steps or epochs as the stopping criterion. Under this practical setting, the conditions of our experiment are meaningful because $T < \infty$ implies $K < \infty$ with a fixed M (therefore, K is a fixed finite value). For these reasons and from our proofs under a practical setting, our theoretical analysis can be used to evaluate the performance of RSGD including calculation of SFO rates under our experimental setting. Thus, our theoretical analysis supports the numerical results.*

5 Conclusion

Our theoretical analysis using several learning rates, including cosine annealing and polynomial decay, demonstrated that using an increasing batch size rather than a constant batch size improves the convergence rate of Riemannian stochastic gradient descent. This finding is supported by our experimental results. Furthermore, increasing batch size yields minimizers that achieve a smaller gradient norm within a shorter computational time owing to improvements in the stochastic first-order oracle rate. These results indicate that increasing batch size combines the advantages of both small and large batch size. However, due to the nature of the experimental tasks, we were unable to investigate its effect on generalization performance. We believe our results, which clarify one facet of the effectiveness of increasing batch size, offer insight into this important problem.

References

- P.-A. Absil, R. Mahony, and R. Sepulchre. *Optimization Algorithms on Matrix Manifolds*. Princeton University Press, 2008.
- Alekh Agarwal and Leon Bottou. A lower bound for the optimization of finite sums. In *Proceedings of the 32nd International Conference on Machine Learning*, 2015.
- Silvère Bonnabel. Stochastic gradient descent on riemannian manifolds. *IEEE Transactions on Automatic Control*, 58(9):2217–2229, 2013.
- Nicolas Boumal. *An introduction to optimization on smooth manifolds*. Cambridge University Press, 2023.
- Nicolas Boumal and P.-A. Absil. Low-rank matrix completion via preconditioned optimization on the grassmann manifold. *Linear Algebra and its Applications*, 475:200–239, 2015.
- Arnaud Breloy, Sandeep Kumar, Ying Sun, and Daniel P. Palomar. Majorization-minimization on the stiefel manifold with application to robust sparse pca. *IEEE Transactions on Signal Processing*, 69:1507–1520, 2021.
- Ines Chami, Zhitao Ying, Christopher Ré, and Jure Leskovec. Hyperbolic graph convolutional neural networks. In *Advances in Neural Information Processing Systems*, 2019.
- Liang-Chieh Chen, George Papandreou, Iasonas Kokkinos, Kevin Murphy, and Alan L. Yuille. Deeplab: Semantic image segmentation with deep convolutional nets, atrous convolution, and fully connected crfs. *IEEE Trans. Pattern Anal. Mach. Intell.*, 40(4):834–848, 2018.
- Xin Chen, Jian Weng, Wei Lu, Jiaming Xu, and Jiasi Weng. Deep manifold learning combined with convolutional neural networks for action recognition. *IEEE transactions on neural networks and learning systems*, 29(9):3938–3952, 2017.
- Christopher Criscitiello and Nicolas Boumal. Curvature and complexity: Better lower bounds for geodesically convex optimization. In *The Thirty Sixth Annual Conference on Learning Theory*, 2023.
- Alain Durmus, Pablo Jiménez, Eric Moulines, and Salem Said. On riemannian stochastic approximation schemes with fixed step-size. In *The 24th International Conference on Artificial Intelligence and Statistics*, 2021.
- Kenneth Y. Goldberg, Theresa Roeder, Dhruv Gupta, and Chris Perkins. Eigentaste: A constant time collaborative filtering algorithm. *Inf. Retr.*, 4(2):133–151, 2001.
- Priya Goyal, Piotr Dollár, Ross B. Girshick, Pieter Noordhuis, Lukasz Wesolowski, Aapo Kyrola, Andrew Tulloch, Yangqing Jia, and Kaiming He. Accurate, large minibatch SGD: training imagenet in 1 hour. *arXiv*, 2017.
- Andi Han and Junbin Gao. Improved variance reduction methods for riemannian non-convex optimization. *IEEE Transactions on Pattern Analysis and Machine Intelligence*, 44(11):7610–7623, 2022.
- F. Maxwell Harper and Joseph A. Konstan. The movielens datasets: History and context. *ACM Trans. Interact. Intell. Syst.*, 5(4):19:1–19:19, 2016.
- Kaiming He, Xiangyu Zhang, Shaoqing Ren, and Jian Sun. Deep residual learning for image recognition. In *2016 IEEE Conference on Computer Vision and Pattern Recognition*, pp. 770–778. IEEE Computer Society, 2016.
- Reshad Hosseini and Suvrit Sra. An alternative to EM for gaussian mixture models: batch and stochastic riemannian optimization. *Math. Program.*, 181(1):187–223, 2020.
- Zhiwu Huang, Chengde Wan, Thomas Probst, and Luc Van Gool. Deep learning on lie groups for skeleton-based action recognition. In *Proceedings of the IEEE conference on computer vision and pattern recognition*, 2017.

-
- Chunlin Ji, Yuhao Fu, and Ping He. Adaptive riemannian stochastic gradient descent and reparameterization for gaussian mixture model fitting. In *Asian Conference on Machine Learning*, 2023.
- Hiroyuki Kasai and Bamdev Mishra. Low-rank tensor completion: a riemannian manifold preconditioning approach. In *Proceedings of the 33rd International Conference on Machine Learning*, 2016.
- Hiroyuki Kasai, Hiroyuki Sato, and Bamdev Mishra. Riemannian stochastic recursive gradient algorithm. In *Proceedings of the 35th International Conference on Machine Learning*, 2018.
- Hiroyuki Kasai, Pratik Jawanpuria, and Bamdev Mishra. Riemannian adaptive stochastic gradient algorithms on matrix manifolds. In *the 36th International Conference on Machine Learning*, 2019.
- Jungbin Kim and Insoon Yang. Nesterov acceleration for riemannian optimization. *arXiv*, 2022.
- Alex Krizhevsky, Ilya Sutskever, and Geoffrey E. Hinton. Imagenet classification with deep convolutional neural networks. In *Advances in Neural Information Processing Systems*, 2012.
- Yann LeCun, Corinna Cortes, and C.J.C. Burges. The mnist database of handwritten digits. <http://yann.lecun.com/exdb/mnist>, 1998.
- Tao Lin, Sebastian U. Stich, Kumar Kshitij Patel, and Martin Jaggi. Don't use large mini-batches, use local SGD. In *8th International Conference on Learning Representations*, 2020a.
- Tianyi Lin, Chenyou Fan, Nhat Ho, Marco Cuturi, and Michael Jordan. Projection robust wasserstein distance and riemannian optimization. In *Advances in Neural Information Processing Systems*, 2020b.
- Changshuo Liu and Nicolas Boumal. Simple algorithms for optimization on riemannian manifolds with constraints. *Applied Mathematics & Optimization*, 2020.
- Qi Liu, Maximilian Nickel, and Douwe Kiela. Hyperbolic graph neural networks. In *Advances in Neural Information Processing Systems*, 2019.
- Yuanyuan Liu, Fanhua Shang, James Cheng, Hong Cheng, and Licheng Jiao. Accelerated first-order methods for geodesically convex optimization on riemannian manifolds. In *Advances in Neural Information Processing Systems*, 2017.
- Ze Liu, Yutong Lin, Yue Cao, Han Hu, Yixuan Wei, Zheng Zhang, Stephen Lin, and Baining Guo. Swin transformer: Hierarchical vision transformer using shifted windows. In *IEEE/CVF International Conference on Computer Vision*, pp. 9992–10002. IEEE, 2021.
- Ilya Loshchilov and Frank Hutter. SGDR: Stochastic gradient descent with warm restarts. In *International Conference on Learning Representations*, 2017.
- Sameer A Nene, Shree K Nayar, Hiroshi Murase, and et al. Columbia object image library (coil-100). Technical report, Columbia University, 1996. CUCS-006-96.
- Luong Trung Nguyen, Junhan Kim, and Byonghyo Shim. Low-rank matrix completion: A contemporary survey. *IEEE Access*, 7:94215–94237, 2019.
- Herbert Robbins and Sutton Monro. A stochastic approximation method. *The Annals of Mathematical Statistics*, 22(3):400–407, 1951.
- Soumava Kumar Roy, Zakaria Mhammedi, and Mehrtash Harandi. Geometry aware constrained optimization techniques for deep learning. In *Proceedings of the IEEE/CVF Conference on Computer Vision and Pattern Recognition*, 2018.
- Walter Rudin. *Principles of Mathematical Analysis (3rd Ed)*. McGraw Hill Higher Education, 1976.
- Hiroyuki Sakai and Hideaki Iiduka. Convergence of riemannian stochastic gradient descent on hadamard manifold. *Pacific Journal of Optimization*, 20(4):743–767, 2024.

-
- Hiroyuki Sakai and Hideaki Iiduka. A general framework of riemannian adaptive optimization methods with a convergence analysis. *Transactions on Machine Learning Research*, 2025.
- Naoki Sato and Hideaki Iiduka. Existence and estimation of critical batch size for training generative adversarial networks with two time-scale update rule. In *International Conference on Machine Learning*, 2023.
- Christopher J. Shallue, Jaehoon Lee, Joseph M. Antognini, Jascha Sohl-Dickstein, Roy Frostig, and George E. Dahl. Measuring the effects of data parallelism on neural network training. *J. Mach. Learn. Res.*, 20: 112:1–112:49, 2019.
- Samuel L. Smith, Pieter-Jan Kindermans, Chris Ying, and Quoc V. Le. Don’t decay the learning rate, increase the batch size. In *6th International Conference on Learning Representations*, 2018.
- Nilesh Tripuraneni, Nicolas Flammarion, Francis Bach, and Michael I. Jordan. Averaging stochastic gradient descent on Riemannian manifolds. In *Proceedings of the 31st Conference On Learning Theory*, 2018.
- Hikaru Umeda and Hideaki Iiduka. Increasing both batch size and learning rate accelerates stochastic gradient descent. *arXiv*, 2024.
- Bart Vandereycken. Low-rank matrix completion by riemannian optimization. *SIAM J. Optim.*, 23(2): 1214–1236, 2013.
- Jiayun Wang, Yubei Chen, Rudrasis Chakraborty, and Stella X Yu. Orthogonal convolutional neural networks. In *Proceedings of the IEEE/CVF conference on computer vision and pattern recognition*, 2020.
- Melanie Weber and Suvrit Sra. Riemannian optimization via frank-wolfe methods. *Math. Program.*, 199(1): 525–556, 2023.
- Guodong Zhang, Lala Li, Zachary Nado, James Martens, Sushant Sachdeva, George E. Dahl, Christopher J. Shallue, and Roger B. Grosse. Which algorithmic choices matter at which batch sizes? insights from a noisy quadratic model. In *Advances in Neural Information Processing Systems*, 2019.
- Hongyi Zhang and Suvrit Sra. First-order methods for geodesically convex optimization. In *Proceedings of the 29th Conference on Learning Theory*, 2016.
- Shichao Zhu, Shirui Pan, Chuan Zhou, Jia Wu, Yanan Cao, and Bin Wang. Graph geometry interaction learning. *Advances in Neural Information Processing Systems*, 2020.

A Calculation of SFO Complexity

A.1 SFO Rates with Constant BS and Increasing BS

We compute the SFO rate required to achieve $\|G_T\|^2 \leq \epsilon^2$ ($\epsilon > 0$), as described in Section 4.3.

[Constant BS]

From Theorem 1, the number of iterations T required to achieve $\|G_T\|^2 \leq \epsilon^2$ is

$$T = \frac{\tilde{Q}_1}{\epsilon^2 - \tilde{Q}_2 \sigma b^{-1}}.$$

Since the SFO complexity of constant BS can be represented by $\text{SFO}(b) = bT$, the $\text{SFO}(b)$ required to achieve $\|G_T\|^2 \leq \epsilon^2$ is given by

$$\text{SFO}_\epsilon(b) = bT = b \frac{\tilde{Q}_1}{\epsilon^2 - \tilde{Q}_2 \sigma b^{-1}} = \frac{b^2 \tilde{Q}_1}{b\epsilon^2 - \tilde{Q}_2 \sigma}.$$

Since

$$\frac{d}{db}\text{SFO}_\epsilon(b) = \frac{2b\tilde{Q}_1(b\epsilon^2 - \tilde{Q}_2\sigma) - b^2\tilde{Q}_1\epsilon^2}{(b\epsilon^2 - \tilde{Q}_2\sigma)^2} = \frac{b\tilde{Q}_1(b\epsilon^2 - 2\tilde{Q}_2\sigma^2)}{(b\epsilon^2 - \tilde{Q}_2\sigma)^2}$$

holds, from

$$b \leq \frac{2\tilde{Q}_2\sigma^2}{\epsilon^2} \Rightarrow \frac{d}{db}\text{SFO}_\epsilon(b) \leq 0 \quad \text{and} \quad b \geq \frac{2\tilde{Q}_2\sigma^2}{\epsilon^2} \Rightarrow \frac{d}{db}\text{SFO}_\epsilon(b) \geq 0,$$

we have the critical batch size of constant BS:

$$b^* := \frac{2\tilde{Q}_2\sigma^2}{\epsilon^2} = \underset{b>0}{\operatorname{argmin}}\text{SFO}_\epsilon(b),$$

which implies

$$\text{SFO}_\epsilon(b^*) = \frac{4\tilde{Q}_1\tilde{Q}_2^2\sigma^4\epsilon^{-4}}{\tilde{Q}_2\sigma^2} = 4\tilde{Q}_1\tilde{Q}_2\sigma^2\epsilon^{-4} = O(\epsilon^{-4}).$$

[Increasing BS]

From Theorem 1, the number of iterations T required to achieve $\|G_T\|^2 \leq \epsilon^2$ is given by

$$T = \frac{\tilde{Q}_1 + \tilde{Q}_2\sigma^2 b_0^{-1}}{\epsilon^2}.$$

We assume a setting in which $T = MK$, meaning that by the T -th iteration, the BS has been increased M times, and RSGD has been updated for K steps at each BS. If the exact value of T takes the form $T = MK + k$ ($1 \leq k \leq K - 1$), we can set T to $M(K + 1)$ to ensure that $\|G_T\|^2 \leq \epsilon^2$ still holds. Similarly, if T takes the form $T = MK - k$ ($1 \leq k \leq K - 1$), we can set T to MK to satisfy the same condition. Hence, our assumption that $T = MK$ is reasonable.

SFO complexity for increasing BS (i.e., exponential growth BS) can be represented as

$$\text{SFO} = \left(\sum_{m=0}^{M-1} b_0\gamma^m \right) K = \frac{b_0}{\gamma - 1} K(\gamma^M - 1).$$

Under our theoretical assumption that K is fixed and M is dynamic, and with $M = \frac{T}{K}$, the SFO complexity of increasing BS for achieving $\|G_T\|^2 \leq \epsilon^2$ is

$$\text{SFO}_\epsilon = \frac{b_0 K}{\gamma - 1} \left(\gamma^{\frac{\tilde{Q}_1 + \tilde{Q}_2\sigma^2 b_0^{-1}}{K\epsilon^2}} - 1 \right) = O(\gamma^{\epsilon^{-2}}).$$

Since \tilde{Q}_2 contains K , as shown by the formal statement of Theorem 2 (with constant LR and exponential growth BS), we rearrange \tilde{Q}_2 for calculating SFO rate under our experimental setting as

$$\tilde{Q}_2 = K\tilde{Q}_3,$$

where \tilde{Q}_3 is defined through this substitution. Then, we obtain

$$MK = T = \frac{\tilde{Q}_1 + \tilde{Q}_2\sigma^2 b_0^{-1}}{\epsilon^2} = \frac{\tilde{Q}_1 + \tilde{Q}_3 K\sigma^2 b_0^{-1}}{\epsilon^2},$$

which implies

$$K = \frac{\tilde{Q}_1}{M\epsilon^2 - \tilde{Q}_3\sigma^2 b_0^{-1}}.$$

Therefore, under our experiment setting—where K is determined by fixed M —and with $K = \frac{T}{M}$, the SFO complexity of increasing BS for achieving $\|G_T\|^2 \leq \epsilon^2$ becomes

$$\text{SFO}_\epsilon = \frac{b_0(\gamma^M - 1)}{\gamma - 1} \frac{\tilde{Q}_1}{M\epsilon^2 - \tilde{Q}_3\sigma^2 b_0^{-1}} = O(\epsilon^{-2}).$$

A.2 Relationship between M the number of increments the BS and the convergence of RSGD

In our numerical experiment in Section 4.3, among the increasing BS configurations, the one with six total BS increases exhibited notably better performance than the one with three increases. We explain this result on the basis of our theoretical analysis. In this section, we assume the same condition as in A.1; namely, $T = MK$. From Theorem 1, we have the following bound for constant and exponential growth BS:

$$\begin{aligned} \min_{t \in \{0, \dots, T-1\}} \mathbb{E}[\|\text{grad}f(x_t)\|_{x_t}^2] &\leq \frac{1}{(2 - L_r \eta_{\max}) \eta_{\max}} \left\{ 2(f(x_0) - f^*) + \frac{L_r \eta_{\max}^2 K \gamma \sigma^2}{\gamma - 1} \frac{1}{b_0} \right\} \frac{1}{T} \\ &= \frac{\tilde{Q}_1}{T} + \tilde{Q}_3 \sigma^2 b_0^{-1} \frac{K}{T} = \frac{\tilde{Q}_1}{T} + \tilde{Q}_3 \sigma^2 b_0^{-1} \frac{1}{M} \\ &= O\left(\frac{1}{T} + \frac{1}{M}\right). \end{aligned}$$

This rate suggests larger M leads to faster convergence rate. From this perspective, it is reasonable that $M = 6$ outperformed $M = 3$ in our numerical experiment.

B Objective Function Value against SFO Complexity

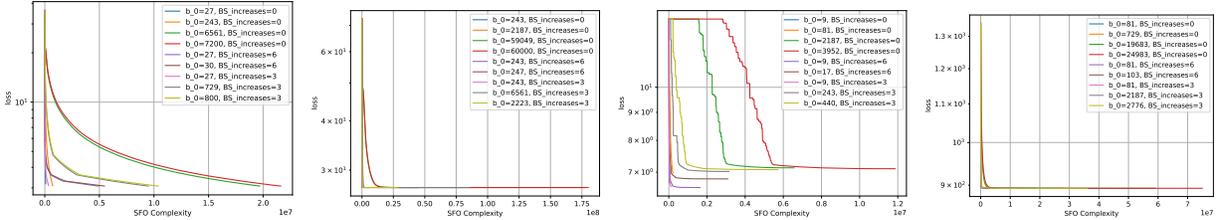


Figure 6: Objective function value against SFO complexity on COIL100 (PCA), MNIST (PCA), MovieLens-1M (LRMC), and Jester (LRMC) in order from left to right.

C Proof of The Propositions

C.1 Proof of Lemma 1

We define $\mathcal{F}_t := \sigma[x_0, (\xi_{j,0})_j, (\xi_{j,1})_j, \dots, (\xi_{j,t-1})_j]$, where x_0 is the initial point of RSGD. For measurable function f , $\mathbb{E}[f|\mathcal{F}_t]$ denotes the conditional expectation of \mathcal{F}_t .

Proof. Considering Assumption 1, we start with

$$f(x_{t+1}) \leq f(x_t) - \eta_t \langle \text{grad}f(x_t), \text{grad}f_{B_t}(x_t) \rangle_{x_t} + \frac{\eta_t^2}{2} L_r \|\text{grad}f_{B_t}(x_t)\|_{x_t}^2,$$

$$\begin{aligned} \mathbb{E}[\|\text{grad}f_{B_t}(x_t)\|_{x_t}^2 | \mathcal{F}_{t+1}] &= \mathbb{E}[\|\text{grad}f_{B_t}(x_t) - \text{grad}f(x_t) + \text{grad}f(x_t)\|_{x_t}^2 | \mathcal{F}_{t+1}] \\ &\leq \mathbb{E}[\|\text{grad}f_{B_t}(x_t) - \text{grad}f(x_t)\|_{x_t}^2 | \mathcal{F}_{t+1}] + \mathbb{E}[\|\text{grad}f(x_t)\|_{x_t}^2 | \mathcal{F}_{t+1}] \\ &\quad + 2\mathbb{E}[\langle \text{grad}f_{B_t}(x_t) - \text{grad}f(x_t), \text{grad}f(x_t) \rangle_{x_t} | \mathcal{F}_{t+1}] \\ &= \mathbb{E}[\|\text{grad}f_{B_t}(x_t) - \text{grad}f(x_t)\|_{x_t}^2 | \mathcal{F}_{t+1}] + \mathbb{E}[\|\text{grad}f(x_t)\|_{x_t}^2 | \mathcal{F}_{t+1}] \\ &\quad + 2\langle \mathbb{E}[\text{grad}f_{B_t}(x_t) | \mathcal{F}_{t+1}] - \text{grad}f(x_t), \text{grad}f(x_t) \rangle_{x_t} \\ &\leq \frac{\sigma^2}{b_t} + \mathbb{E}[\|\text{grad}f(x_t)\|_{x_t}^2 | \mathcal{F}_{t+1}] \quad \text{a.s.}, \end{aligned}$$

and

$$\mathbb{E}[\langle \text{grad}f(x_t), \text{grad}f_{B_t}(x_t) \rangle_{x_t} | \mathcal{F}_{t+1}] = \langle \text{grad}f(x_t), \mathbb{E}[\text{grad}f_{B_t}(x_t) | \mathcal{F}_{t+1}]_{x_t} \rangle = \|\text{grad}f(x_t)\|_{x_t}^2 \quad \text{a.s.}$$

Taking the total expectation for the above equations, we have

$$\begin{aligned} \mathbb{E}[f(x_{t+1})] &\leq \mathbb{E}[f(x_t)] - \eta_t \mathbb{E}[\langle \text{grad}f(x_t), \text{grad}f_{B_t}(x_t) \rangle_{x_t}] + \frac{\eta_t^2}{2} L_r \mathbb{E}[\|\text{grad}f_{B_t}(x_t)\|_{x_t}^2] \\ &= \mathbb{E}[f(x_t)] - \eta_t \mathbb{E}[\mathbb{E}[\langle \text{grad}f(x_t), \text{grad}f_{B_t}(x_t) \rangle_{x_t} | \mathcal{F}_{t+1}]] + \frac{\eta_t^2}{2} L_r \mathbb{E}[\mathbb{E}[\|\text{grad}f_{B_t}(x_t)\|_{x_t}^2 | \mathcal{F}_{t+1}]] \\ &\leq \mathbb{E}[f(x_t)] - \eta_t \mathbb{E}[\|\text{grad}f(x_t)\|_{x_t}^2] + \frac{\eta_t^2 L_r}{2} \left(\frac{\sigma^2}{b_t} + \mathbb{E}[\|\text{grad}f(x_t)\|_{x_t}^2] \right) \\ &= \mathbb{E}[f(x_t)] + \frac{L_r \sigma^2 \eta_t^2}{2b_t} - \eta_t \left(1 - \frac{L_r \eta_t}{2} \right) \mathbb{E}[\|\text{grad}f(x_t)\|_{x_t}^2]. \end{aligned}$$

□

C.2 Proof of Lemma 2

Proof. Taking $\eta_{\max} < \frac{2}{L_r}$ into consideration, we start with

$$\sum_{t=0}^{T-1} \eta_t \left(1 - \frac{L_r \eta_t}{2} \right) \mathbb{E}[\|\text{grad}f(x_t)\|_{x_t}^2] \geq \left(1 - \frac{L_r \eta_{\max}}{2} \right) \min_{t \in \{0, \dots, T-1\}} \mathbb{E}[\|\text{grad}f(x_t)\|_{x_t}^2] \sum_{t=0}^{T-1} \eta_t.$$

By taking the summation on both sides of the inequality for Lemma 1 and evaluating it using the above inequality, we obtain

$$\begin{aligned} &\left(1 - \frac{L_r \eta_{\max}}{2} \right) \min_{t \in \{0, \dots, T-1\}} \mathbb{E}[\|\text{grad}f(x_t)\|_{x_t}^2] \sum_{t=0}^{T-1} \eta_t \\ &\leq \sum_{t=0}^{T-1} \eta_t \left(1 - \frac{L_r \eta_t}{2} \right) \mathbb{E}[\|\text{grad}f(x_t)\|_{x_t}^2] \\ &\leq \sum_{t=0}^{T-1} (\mathbb{E}[f(x_t)] - \mathbb{E}[f(x_{t+1})]) + \sum_{t=0}^{T-1} \frac{L_r \sigma^2 \eta_t^2}{2b_t} = \mathbb{E}[f(x_0) - f(x_T)] + \sum_{t=0}^{T-1} \frac{L_r \sigma^2 \eta_t^2}{2b_t}. \end{aligned}$$

$(\mathbb{E}[f(x_t)])_{t \in \{0, \dots, T\}}$ being a decreasing sequence implies

$$\mathbb{E}[f(x_0) - f(x_T)] \leq \mathbb{E}[f(x_0) - f^*] = f(x_0) - f^*.$$

Therefore,

$$\min_{t \in \{0, \dots, T-1\}} \mathbb{E}[\|\text{grad}f(x_t)\|_{x_t}^2] \leq \frac{2(f(x_0) - f^*)}{2 - L_r \eta_{\max}} \frac{1}{\sum_{t=0}^{T-1} \eta_t} + \frac{L_r \sigma^2}{2 - L_r \eta_{\max}} \frac{1}{\sum_{t=0}^{T-1} \eta_t} \sum_{t=0}^{T-1} \frac{\eta_t^2}{b_t}.$$

□

C.3 Proof of Theorem 1

Proof. We set $b_t = b$ in Lemma 2.

[Constant LR equation 1]

From Lemma 2, we have

$$\sum_{t=0}^{T-1} \eta_t = \sum_{t=0}^{T-1} \eta_{\max} = \eta_{\max} T, \quad \sum_{t=0}^{T-1} \frac{\eta_t^2}{b_t} = \frac{1}{\sum_{t=0}^{T-1} \eta_{\max}} \sum_{t=0}^{T-1} \frac{\eta_{\max}^2}{b} = \frac{\eta_{\max}^2}{b} T,$$

which imply

$$\min_{t \in \{0, \dots, T-1\}} \mathbb{E}[\|\text{grad}f(x_t)\|_{x_t}^2] \leq \frac{2(f(x_0) - f^*)}{(2 - L_r \eta_{\max}) \eta_{\max} T} + \frac{L_r \eta_{\max}}{2 - L_r \eta_{\max}} \frac{\sigma^2}{b}.$$

[Diminishing LR equation 2]

From Lemma 2, we have

$$\sum_{t=0}^{T-1} \eta_t = \eta_{\max} \sum_{t=0}^{T-1} \frac{1}{\sqrt{t+1}} \geq \eta_{\max} \sum_{t=0}^{T-1} \frac{1}{\sqrt{T}} = \eta_{\max} \frac{T}{\sqrt{T}} = \eta_{\max} \sqrt{T}$$

and

$$\sum_{t=0}^{T-1} \frac{\eta_t^2}{b_t} = \frac{\eta_{\max}^2}{b} \sum_{t=0}^{T-1} \frac{1}{t+1} \leq \frac{\eta_{\max}^2}{b} \left(1 + \int_1^T \frac{dt}{t} \right) = \frac{\eta_{\max}^2}{b} + \frac{\eta_{\max}^2}{b} \log T,$$

which imply

$$\min_{t \in \{0, \dots, T-1\}} \mathbb{E}[\|\text{grad}f(x_t)\|_{x_t}^2] \leq \frac{f(x_0) - f^*}{(2 - L_r \eta_{\max}) \eta_{\max} \sqrt{T}} + \frac{L_r \eta_{\max}}{2 - L_r \eta_{\max}} \frac{\sigma^2}{b} \frac{1 + \log T}{\sqrt{T}}.$$

[Cosine Annealing LR equation 3]

From Lemma 2, we have

$$\begin{aligned} \sum_{t=0}^{T-1} \eta_t &\geq \int_0^T \eta_t dt = \frac{\eta_{\max} + \eta_{\min}}{2} T + \frac{\eta_{\max} - \eta_{\min}}{2} \int_0^T \cos\left(\frac{t}{T}\pi\right) dt \\ &= \frac{\eta_{\max} + \eta_{\min}}{2} T \end{aligned}$$

and

$$\begin{aligned} \sum_{t=0}^{T-1} \eta_t^2 &= \frac{(\eta_{\max} + \eta_{\min})^2}{4} T + \frac{\eta_{\max}^2 + \eta_{\min}^2}{2} \sum_{t=0}^{T-1} \cos \frac{t}{T} \pi + \frac{(\eta_{\max} - \eta_{\min})^2}{4} \sum_{t=0}^{T-1} \cos^2 \frac{t}{T} \pi \\ &\leq \frac{(\eta_{\max} + \eta_{\min})^2}{4} T + \frac{\eta_{\max}^2 - \eta_{\min}^2}{2} T + \frac{(\eta_{\max} - \eta_{\min})^2}{4} T \\ &= \eta_{\max}^2 T, \end{aligned}$$

which imply

$$\min_{t \in \{0, \dots, T-1\}} \mathbb{E}[\|\text{grad}f(x_t)\|_{x_t}^2] \leq \frac{4(f(x_0) - f^*)}{(2 - L_r \eta_{\max})(\eta_{\max} + \eta_{\min})} \frac{1}{T} + \frac{2L_r \eta_{\max}^2}{(2 - L_r \eta_{\max})(\eta_{\max} + \eta_{\min})} \frac{\sigma^2}{b}.$$

[Polynomial Decay LR equation 4]

We start by recalling the Riemann integral (e.g., Rudin (1976)) of $g(t) := (1 - t)^p \geq 0 (0 \leq t \leq 1)$. $U(P_T) := \sum_{t=0}^{T-1} \frac{1}{T} (1 - \frac{t}{T})^p$ is an upper Riemann sum with the function g and a partition $P_T := \{0, \frac{1}{T}, \dots, \frac{T-1}{T}, 1\}$ due to g being monotone decreasing. From the definition of an Riemann integral (e.g., Rudin (1976, Section 6)), if $\int_0^1 g(t) dt$ exists, then

$$\inf_{P: \text{Partitions of } [0,1]} U(P) = \int_0^1 g(t) dt.$$

In fact, the integral value exists. Thus, we obtain

$$\sum_{t=0}^{T-1} \frac{1}{T} \left(1 - \frac{t}{T}\right)^p = U(P_T) \geq \inf_{P: \text{Partitions of } [0,1]} U(P) = \int_0^1 (1 - t)^p dt = \frac{1}{p+1}.$$

Similarly, if we define $L(P_T)$ as $\sum_{t=1}^T \frac{1}{T} \left(1 - \frac{t}{T}\right)^p$, then $L(P_T)$ is a lower Riemann sum with the function g and a partition P_T , and the supremum of $L(P_T)$ equals $\int_0^1 g(t)dt$. Considering

$$\sum_{t=0}^{T-1} \frac{1}{T} \left(1 - \frac{t}{T}\right)^p = L(P_T) + \frac{1}{T},$$

we have

$$\sum_{t=0}^{T-1} \frac{1}{T} \left(1 - \frac{t}{T}\right)^p = L(P_T) + \frac{1}{T} \leq \sup_{P: \text{Partitions of } [0,1]} L(P) + \frac{1}{T} = \int_0^1 (1-t)^p dt + \frac{1}{T} = \frac{1}{p+1} + \frac{1}{T}.$$

Hence,

$$\frac{T}{p+1} \leq \sum_{t=0}^{T-1} \left(1 - \frac{t}{T}\right)^p \leq \frac{T}{p+1} + 1$$

holds. By replacing g with $(1+t)^{2p}$ ($0 \leq t \leq 1$) and using the same logic, we obtain

$$\sum_{t=0}^{T-1} \frac{1}{T} \left(1 - \frac{t}{T}\right)^{2p} \leq \int_0^1 (1-t)^{2p} dt + \frac{1}{T} = \frac{1}{2p+1} + \frac{1}{T}.$$

Therefore, considering Lemma 2,

$$\begin{aligned} \sum_{t=0}^{T-1} \eta_t &= \eta_{\min} T + (\eta_{\max} - \eta_{\min}) \sum_{t=0}^{T-1} \left(1 - \frac{t}{T}\right)^p \\ &\geq \eta_{\min} T + (\eta_{\max} - \eta_{\min}) \frac{T}{p+1} = \frac{\eta_{\max} + p\eta_{\min}}{p+1} T, \end{aligned}$$

and

$$\begin{aligned} \sum_{t=0}^{T-1} \eta_t^2 &= \eta_{\min} T + 2\eta_{\min}(\eta_{\max} - \eta_{\min}) \sum_{t=0}^{T-1} \left(1 - \frac{t}{T}\right)^p + (\eta_{\max} - \eta_{\min})^2 \sum_{t=0}^{T-1} \left(1 - \frac{t}{T}\right)^{2p} \\ &\leq \eta_{\min} T + 2\eta_{\min}(\eta_{\max} - \eta_{\min}) \left(1 + \frac{T}{p+1}\right) + (\eta_{\max} - \eta_{\min})^2 \left(1 + \frac{T}{2p+1}\right) \\ &= \eta_{\max}^2 - \eta_{\min}^2 + \left(\eta_{\min} + \frac{2\eta_{\min}(\eta_{\max} - \eta_{\min})}{p+1} + \frac{(\eta_{\max} - \eta_{\min})^2}{2p+1}\right) T, \end{aligned}$$

we have

$$\begin{aligned} &\min_{t \in \{0, \dots, T-1\}} \mathbb{E}[\|\text{grad}f(x_t)\|_{x_t}^2] \\ &\leq \frac{p+1}{(2 - L_r \eta_{\max})(\eta_{\max} + p\eta_{\min})} \left\{ 2(f(x_0) - f^*) + \frac{L_r(\eta_{\max}^2 - \eta_{\min}^2)\sigma^2}{b} \right\} \frac{1}{T} \\ &\quad + \frac{L_r(p+1)(\eta_{\max}^2 - \eta_{\min}^2)}{(2 - L_r \eta_{\max})(\eta_{\max} + p\eta_{\min})} \left(\eta_{\min} + \frac{2\eta_{\min}(\eta_{\max} - \eta_{\min})}{p+1} + \frac{(\eta_{\max} - \eta_{\min})^2}{2p+1} \right) \frac{\sigma^2}{b}. \end{aligned}$$

□

C.4 Proof of Theorem 2

Proof. The evaluations in all these cases are based on Lemma 2 and use estimations of $\sum_{t=0}^{T-1} \eta_t$ in the proof of Theorem 1.

[Exponential Growth BS equation 5 and Constant LR equation 1]

From the fact that sums of positive term series are the supremum of their finite sums, we have

$$\sum_{t=0}^{T-1} \frac{1}{b_t} = \sum_{m=0}^{M-1} \frac{K}{b_0 \gamma^m} + \frac{T-KM}{b_0 \gamma^M} \leq \sum_{m=0}^M \frac{K}{b_0 \gamma^m} \leq \frac{K}{b_0} \sum_{m=0}^{\infty} \frac{1}{\gamma^m} = \frac{K\gamma}{b_0(\gamma-1)}, \quad (9)$$

which implies

$$\sum_{t=0}^{T-1} \frac{\eta_{\max}^2}{b_t} = \eta_{\max}^2 \sum_{t=0}^{T-1} \frac{1}{b_t} \leq \frac{\eta_{\max}^2 K\gamma}{b_0(\gamma-1)}.$$

Therefore,

$$\min_{t \in \{0, \dots, T-1\}} \mathbb{E}[\|\text{grad}f(x_t)\|_{x_t}^2] \leq \frac{1}{(2 - L_r \eta_{\max}) \eta_{\max}} \left\{ 2(f(x_0) - f^*) + \frac{L_r \eta_{\max}^2 K\gamma \sigma^2}{\gamma - 1} \frac{1}{b_0} \right\} \frac{1}{T}.$$

[Exponential Growth BS equation 5 and Diminishing LR equation 2]

Using equation 9, we have

$$\sum_{t=0}^{T-1} \frac{\eta_t^2}{b_t} = \eta_{\max}^2 \sum_{t=0}^{T-1} \frac{1}{(t+1)b_t} \leq \eta_{\max}^2 \sum_{t=0}^{T-1} \frac{1}{b_t} \leq \frac{\eta_{\max}^2 K\gamma}{b_0(\gamma-1)},$$

which implies

$$\min_{t \in \{0, \dots, T-1\}} \mathbb{E}[\|\text{grad}f(x_t)\|_{x_t}^2] \leq \frac{1}{(2 - L_r \eta_{\max}) \eta_{\max}} \left\{ 2(f(x_0) - f^*) + \frac{L_r \eta_{\max}^2 K\gamma \sigma^2}{\gamma - 1} \frac{1}{b_0} \right\} \frac{1}{\sqrt{T}}.$$

[Exponential Growth BS equation 5 and Cosine Annealing LR equation 3]

From equation 9 and $|\cos x| \leq 1$, we have

$$\begin{aligned} \sum_{t=0}^{T-1} \frac{\eta_t^2}{b_t} &= \sum_{t=0}^{T-1} \frac{1}{b_t} \left(\frac{(\eta_{\max} + \eta_{\min})^2}{4} + \frac{(\eta_{\max} - \eta_{\min})^2}{4} \cos^2 \frac{t}{T} \pi + \frac{\eta_{\max}^2 - \eta_{\min}^2}{2} \cos \frac{t}{T} \pi \right) \\ &\leq \eta_{\max}^2 \sum_{t=0}^{T-1} \frac{1}{b_t} \leq \frac{\eta_{\max}^2 K\gamma}{b_0(\gamma-1)}, \end{aligned}$$

which implies

$$\min_{t \in \{0, \dots, T-1\}} \mathbb{E}[\|\text{grad}f(x_t)\|_{x_t}^2] \leq \frac{2}{(2 - L_r \eta_{\max})(\eta_{\max} + \eta_{\min})} \left\{ 2(f(x_0) - f^*) + \frac{L_r \eta_{\max}^2 K\gamma \sigma^2}{\gamma - 1} \frac{1}{b_0} \right\} \frac{1}{T}.$$

[Exponential Growth BS equation 5 and Polynomial Decay LR equation 4]

From equation 9 and $t \leq T$, we have

$$\begin{aligned} \sum_{t=0}^{T-1} \frac{\eta_t^2}{b_t} &= \sum_{t=0}^{T-1} \frac{1}{b_t} \left\{ \eta_{\min}^2 + (\eta_{\max} - \eta_{\min})^2 \left(1 - \frac{t}{T}\right)^{2p} + 2\eta_{\min}(\eta_{\max} - \eta_{\min}) \left(1 - \frac{t}{T}\right)^p \right\} \\ &\leq \eta_{\max}^2 \sum_{t=0}^{T-1} \frac{1}{b_t} \leq \frac{\eta_{\max}^2 K\gamma}{b_0(\gamma-1)}, \end{aligned}$$

which implies

$$\min_{t \in \{0, \dots, T-1\}} \mathbb{E}[\|\text{grad}f(x_t)\|_{x_t}^2] \leq \frac{p+1}{(2 - L_r \eta_{\max})(\eta_{\max} + p\eta_{\min})} \left\{ 2(f(x_0) - f^*) + \frac{L_r \eta_{\max}^2 K\gamma \sigma^2}{\gamma - 1} \frac{1}{b_0} \right\} \frac{1}{T}.$$

[Polynomial Growth BS equation 6 and Constant LR equation 1]

We set $\underline{a} := a \wedge b_0$. Considering $c > 1$, we have

$$\begin{aligned} \sum_{t=0}^{T-1} \frac{1}{b_t} &= \sum_{m=0}^{M-1} \frac{K}{(am + b_0)^c} + \frac{T - KM}{(aM + b_0)^c} \leq \sum_{m=0}^M \frac{K}{(am + b_0)^c} \leq \frac{K}{\underline{a}^{[c]}} \sum_{m=0}^M \frac{1}{(m+1)^c} \\ &= \frac{K}{\underline{a}^{[c]}} \sum_{m=1}^{\infty} \frac{1}{m^c} = \frac{K\zeta(c)}{\underline{a}^{[c]}}, \end{aligned} \quad (10)$$

which implies

$$\sum_{t=0}^{T-1} \frac{\eta_t^2}{b_t} = \eta_{\max}^2 \sum_{t=0}^{T-1} \frac{1}{b_t} \leq \frac{\eta_{\max}^2 K\zeta(c)}{\underline{a}^{[c]}}.$$

Therefore,

$$\min_{t \in \{0, \dots, T-1\}} \mathbb{E}[\|\text{grad}f(x_t)\|_{x_t}^2] \leq \frac{1}{(2 - L_r \eta_{\max}) \eta_{\max}} \left(2(f(x_0) - f^*) + \frac{L_r \eta_{\max}^2 K\zeta(c) \sigma^2}{\underline{a}^{[c]}} \right) \frac{1}{T},$$

where, for $c > 1$, Riemann zeta function $\zeta(c) < \infty$; $\zeta(c)$ is monotone decreasing on $c \in (1, \infty)$ and $\lim_{c \rightarrow \infty} \zeta(c) = 1$.

[Polynomial Growth BS equation 6 and Diminishing LR equation 2]

From equation 10, we have

$$\sum_{t=0}^{T-1} \frac{\eta_t^2}{b_t} = \eta_{\max}^2 \sum_{t=0}^{T-1} \frac{1}{(t+1)b_t} \leq \eta_{\max}^2 \sum_{t=0}^{T-1} \frac{1}{b_t} \leq \frac{\eta_{\max}^2 K\zeta(c)}{\underline{a}^{[c]}},$$

which implies

$$\min_{t \in \{0, \dots, T-1\}} \mathbb{E}[\|\text{grad}f(x_t)\|_{x_t}^2] \leq \frac{1}{(2 - L_r \eta_{\max}) \eta_{\max}} \left(2(f(x_0) - f^*) + \frac{L_r \eta_{\max}^2 K\zeta(c) \sigma^2}{\underline{a}^{[c]}} \right) \frac{1}{\sqrt{T}}.$$

[Polynomial Growth BS equation 6 and Cosine Annealing LR equation 3]

From equation 10 and the previous analysis for Cosine Annealing LR equation 3, we have

$$\sum_{t=0}^{T-1} \frac{\eta_t^2}{b_t} \leq \eta_{\max}^2 \sum_{t=0}^{T-1} \frac{1}{b_t} \leq \frac{\eta_{\max}^2 K\zeta(c)}{\underline{a}^{[c]}},$$

which implies

$$\min_{t \in \{0, \dots, T-1\}} \mathbb{E}[\|\text{grad}f(x_t)\|_{x_t}^2] \leq \frac{2}{(2 - L_r \eta_{\max})(\eta_{\max} + \eta_{\min})} \left(2(f(x_0) - f^*) + \frac{L_r \eta_{\max}^2 K\zeta(c) \sigma^2}{\underline{a}^{[c]}} \right) \frac{1}{T}.$$

[Polynomial Growth BS equation 6 and Polynomial Decay LR equation 4]

From equation 10 and the previous analysis for Polynomial Decay LR equation 4, we have

$$\sum_{t=0}^{T-1} \frac{\eta_t^2}{b_t} \leq \eta_{\max}^2 \sum_{t=0}^{T-1} \frac{1}{b_t} \leq \frac{\eta_{\max}^2 K\zeta(c)}{\underline{a}^{[c]}},$$

which implies

$$\min_{t \in \{0, \dots, T-1\}} \mathbb{E}[\|\text{grad}f(x_t)\|_{x_t}^2] \leq \frac{p+1}{(2 - L_r \eta_{\max})(\eta_{\max} + p\eta_{\min})} \left(2(f(x_0) - f^*) + \frac{L_r \eta_{\max}^2 K\zeta(c) \sigma^2}{\underline{a}^{[c]}} \right) \frac{1}{T}.$$

□

C.5 Proof of Theorem 3

Proof. The evaluations in all these cases are based on Lemma 2. We start with an exponential growth BS and a warm-up LR. From $l, l_w \in \mathbb{N}$ and $l_w \geq l$, there exist $\alpha, \beta \in \mathbb{N} \cup \{0\}$ such that $l_w = \alpha l + \beta$. Note that we define summations from 0 to -1 as 0. Furthermore, from $\forall u, v > 0 : 0 \leq u^2 + v^2 + uv$ holds.

[LR Decay Part: Constant equation 1]

Considering $T_w = l_w K' = \alpha(lK') + \beta K'$, we have

$$\sum_{t=T_w}^{T-1} \eta_t = \sum_{t=T_w}^{T-1} \eta_{\max} = (T - T_w)\eta_{\max}$$

and

$$\sum_{t=T_w}^{T-1} \frac{\eta_t^2}{b_t} = \sum_{t=l_w K'}^{(\alpha+1)l-1} \frac{\eta_{\max}^2}{b_t} + \sum_{t=(\alpha+1)l}^{T-1} \frac{\eta_{\max}^2}{b_t} = \sum_{t=T_w}^{T-1} \frac{\eta_{\max}^2}{b_t} \leq \frac{\eta_{\max}^2 K}{b_0} \sum_{m=0}^M \frac{1}{\gamma^m} \leq \frac{\eta_{\max}^2 K}{b_0} \sum_{m=0}^{\infty} \frac{1}{\gamma^m} = \frac{\eta_{\max}^2 \gamma K}{(\gamma - 1)b_0},$$

which imply

$$\min_{t \in \{T_w, \dots, T-1\}} \mathbb{E}[\|\text{grad}f(x_t)\|_{x_t}^2] \leq \frac{1}{(2 - L_r \eta_{\max})\eta_{\max}} \left(2(f(x_0) - f^*) + \frac{L_r \eta_{\max}^2 K \gamma \sigma^2}{\gamma - 1} \frac{1}{b_0} \right) \frac{1}{T - T_w}.$$

[LR Decay Part: Diminishing equation 2]

Similarly, we have

$$\sum_{t=T_w}^{T-1} \eta_t = \sum_{t=T_w}^{T-1} \frac{\eta_{\max}}{\sqrt{t+1}} \geq \eta_{\max} \int_{T_w}^T \frac{dt}{\sqrt{t+1}} = 2\eta_{\max}(\sqrt{T+1} - \sqrt{T_w+1})$$

and

$$\sum_{t=0}^{T-1} \frac{\eta_t^2}{b_t} \leq \sum_{t=T_w}^{T-1} \frac{\eta_{\max}^2}{b_t(t+1)} \leq \sum_{t=T_w}^{T-1} \frac{\eta_{\max}^2}{b_t} \leq \frac{\eta_{\max}^2 \gamma K}{(\gamma - 1)b_0},$$

which imply

$$\min_{t \in \{T_w, \dots, T-1\}} \mathbb{E}[\|\text{grad}f(x_t)\|_{x_t}^2] \leq \frac{1}{2(2 - L_r \eta_{\max})\eta_{\max}} \left(2(f(x_0) - f^*) + \frac{L_r \eta_{\max}^2 K \gamma \sigma^2}{\gamma - 1} \frac{1}{b_0} \right) \frac{1}{\sqrt{T+1} - \sqrt{T_w+1}}.$$

[LR Decay Part: Cosine Annealing equation 3]

We have

$$\begin{aligned} \sum_{t=T_w}^{T-1} \eta_t &= \sum_{t=T_w}^{T-1} \left(\frac{\eta_{\max} + \eta_{\min}}{2} + \frac{\eta_{\max} - \eta_{\min}}{2} \cos \frac{t - T_w}{T - T_w} \pi \right) \\ &= \frac{\eta_{\max} + \eta_{\min}}{2} (T - T_w) + \frac{\eta_{\max} - \eta_{\min}}{2} \sum_{t=T_w}^{T-1} \cos \frac{t - T_w}{T - T_w} \pi \\ &\geq \frac{\eta_{\max} + \eta_{\min}}{2} (T - T_w) + \frac{\eta_{\max} - \eta_{\min}}{2} \int_{T_w}^T \cos \left(\frac{t - T_w}{T - T_w} \pi \right) dt = \frac{\eta_{\max} + \eta_{\min}}{2} (T - T_w) \end{aligned}$$

and

$$\begin{aligned} \sum_{t=T_w}^{T-1} \frac{\eta_t^2}{b_t} &\leq \sum_{t=T_w}^{T-1} \frac{1}{b_t} \left(\frac{(\eta_{\max} + \eta_{\min})^2}{4} + \frac{\eta_{\max}^2 - \eta_{\min}^2}{2} \cos \frac{t - T_w}{T - T_w} \pi + \frac{(\eta_{\max} - \eta_{\min})^2}{4} \cos^2 \frac{t - T_w}{T - T_w} \pi \right) \\ &\leq \sum_{t=0}^{T-1} \frac{1}{b_t} \left(\frac{(\eta_{\max} + \eta_{\min})^2}{4} + \frac{\eta_{\max}^2 - \eta_{\min}^2}{2} + \frac{(\eta_{\max} - \eta_{\min})^2}{4} \right) = \sum_{t=0}^{T-1} \frac{\eta_{\max}^2}{b_t} \leq \frac{\eta_{\max}^2 \gamma K}{(\gamma - 1)b_0}, \end{aligned}$$

which imply

$$\min_{t \in \{T_w, \dots, T-1\}} \mathbb{E}[\|\text{grad}f(x_t)\|_{x_t}^2] \leq \frac{2}{(2 - L_r \eta_{\max})(\eta_{\max} + \eta_{\min})} \left(2(f(x_0) - f^*) + \frac{L_r \eta_{\max}^2 K \gamma \sigma^2}{\gamma - 1} \frac{1}{b_0} \right) \frac{1}{T - T_w}.$$

[LR Decay Part: Polynomial Decay equation 4]

As with the proof of polynomial decay LR equation 4 in Theorem 1, we have

$$\begin{aligned} \sum_{t=T_w}^{T-1} \eta_t &= \sum_{t=T_w}^{T-1} \left\{ \eta_{\min} + (\eta_{\max} - \eta_{\min}) \left(1 - \frac{t - T_w}{T - T_w} \right)^p \right\} \\ &\geq \eta_{\min}(T - T_w) + (\eta_{\max} - \eta_{\min}) \frac{T - T_w}{p + 1} = \frac{\eta_{\max} + p\eta_{\min}}{p + 1} (T - T_w) \end{aligned}$$

and

$$\begin{aligned} \sum_{t=T_w}^{T-1} \frac{\eta_t^2}{b_t} &\leq \sum_{t=T_w}^{T-1} \frac{1}{b_t} \left(\eta_{\min}^2 + (\eta_{\max} - \eta_{\min})^2 \left(1 - \frac{t - T_w}{T - T_w} \right)^{2p} + 2\eta_{\min}(\eta_{\max} - \eta_{\min}) \left(1 - \frac{t - T_w}{T - T_w} \right)^p \right) \\ &\leq \sum_{t=T_w}^{T-1} \frac{\eta_{\max}^2}{b_t} \leq \frac{\eta_{\max}^2 \gamma K}{(\gamma - 1)b_0}, \end{aligned}$$

which imply

$$\min_{t \in \{T_w, \dots, T-1\}} \mathbb{E}[\|\text{grad}f(x_t)\|_{x_t}^2] \leq \frac{p + 1}{(2 - L_r \eta_{\max})(\eta_{\max} + p\eta_{\min})} \left(2(f(x_0) - f^*) + \frac{L_r \eta_{\max}^2 K \gamma \sigma^2}{\gamma - 1} \frac{1}{b_0} \right) \frac{1}{T - T_w}.$$

On the other hand, we consider a polynomial growth BS and a warm-up LR.

[LR Decay Part: Constant equation 1]

We have

$$\sum_{t=T_w}^{T-1} \eta_t = \sum_{t=T_w}^{T-1} \eta_{\max} = \eta_{\max}(T - T_w)$$

and

$$\sum_{t=T_w}^{T-1} \frac{\eta_t^2}{b_t} = \sum_{t=l_w K'}^{(\alpha+1)l-1} \frac{\eta_{\max}^2}{b_t} + \sum_{t=T_w}^{T-1} \frac{\eta_{\max}^2}{b_t} = \sum_{t=T_w}^{T-1} \frac{\eta_{\max}^2}{b_t} \leq \frac{\eta_{\max}^2 K}{\underline{a}^{[c]}} \sum_{m=0}^{M-1} \frac{1}{(m+1)^c} \leq \frac{\eta_{\max}^2 K}{\underline{a}^{[c]}} \sum_{m=1}^{\infty} \frac{1}{m^c} = \frac{\eta_{\max}^2 K \zeta(c)}{\underline{a}^{[c]}}$$

which imply

$$\min_{t \in \{T_w, \dots, T-1\}} \mathbb{E}[\|\text{grad}f(x_t)\|_{x_t}^2] \leq \frac{1}{(2 - L_r \eta_{\max})\eta_{\max}} \left(2(f(x_0) - f^*) + \frac{L_r \eta_{\max}^2 K \zeta(c) \sigma^2}{\underline{a}^{[c]}} \right) \frac{1}{T - T_w}.$$

[LR Decay Part: Diminishing equation 2]

Similarly, we have

$$\sum_{t=T_w}^{T-1} \eta_t = \sum_{t=T_w}^{T-1} \frac{\eta_{\max}}{\sqrt{t+1}} \geq \eta_{\max} \int_{T_w}^T \frac{dt}{\sqrt{t+1}} = 2\eta_{\max}(\sqrt{T+1} - \sqrt{T_w+1})$$

and

$$\sum_{t=T_w}^{T-1} \frac{\eta_t^2}{b_t} = \sum_{t=T_w}^{T-1} \frac{\eta_{\max}^2}{b_t(t+1)} \leq \sum_{t=T_w}^{T-1} \frac{\eta_{\max}^2}{b_t} \leq \frac{\eta_{\max}^2 K \zeta(c)}{\underline{a}^{[c]}}$$

which imply

$$\min_{t \in \{T_w, \dots, T-1\}} \mathbb{E}[\|\text{grad}f(x_t)\|_{x_t}^2] \leq \frac{1}{2(2 - L_r \eta_{\max}) \eta_{\max}} \left(2(f(x_0) - f^*) + \frac{L_r \eta_{\max}^2 K \zeta(c) \sigma^2}{\underline{a}^{\lfloor c \rfloor}} \right) \frac{1}{\sqrt{T+1} - \sqrt{T_w+1}}.$$

[LR Decay Part: Cosine Annealing equation 3]

We have

$$\begin{aligned} \sum_{t=T_w}^{T-1} \eta_t &= \sum_{t=T_w}^{T-1} \left(\frac{\eta_{\max} + \eta_{\min}}{2} + \frac{\eta_{\max} - \eta_{\min}}{2} \cos \frac{t - T_w}{T - T_w} \pi \right) \\ &\geq \frac{\eta_{\max} + \eta_{\min}}{2} (T - T_w) + \frac{\eta_{\max} - \eta_{\min}}{2} \int_{T_w}^T \cos \left(\frac{t - T_w}{T - T_w} \pi \right) dt = \frac{\eta_{\max} + \eta_{\min}}{2} (T - T_w) \end{aligned}$$

and

$$\begin{aligned} \sum_{t=T_w}^{T-1} \frac{\eta_t^2}{b_t} &= \sum_{t=T_w}^{T-1} \frac{1}{b_t} \left(\frac{(\eta_{\max} + \eta_{\min})^2}{4} + \frac{\eta_{\max}^2 - \eta_{\min}^2}{2} \cos \frac{t - T_w}{T - T_w} \pi + \frac{(\eta_{\max} - \eta_{\min})^2}{4} \cos^2 \frac{t - T_w}{T - T_w} \pi \right) \\ &\leq \sum_{t=T_w}^{T-1} \frac{1}{b_t} \left(\frac{(\eta_{\max} + \eta_{\min})^2}{4} + \frac{\eta_{\max}^2 - \eta_{\min}^2}{2} + \frac{(\eta_{\max} - \eta_{\min})^2}{4} \right) = \sum_{t=T_w}^{T-1} \frac{\eta_{\max}^2}{b_t} \leq \frac{\eta_{\max}^2 K \zeta(c)}{\underline{a}^{\lfloor c \rfloor}}, \end{aligned}$$

which imply

$$\min_{t \in \{T_w, \dots, T-1\}} \mathbb{E}[\|\text{grad}f(x_t)\|_{x_t}^2] \leq \frac{2}{(2 - L_r \eta_{\max})(\eta_{\max} + \eta_{\min})} \left(2(f(x_0) - f^*) + \frac{L_r \eta_{\max}^2 K \zeta(c) \sigma^2}{\underline{a}^{\lfloor c \rfloor}} \right) \frac{1}{T - T_w}.$$

[LR Decay Part: Polynomial Decay equation 4]

Considering the proof of Polynomial Decay LR equation 4 in Theorem 1, we have

$$\begin{aligned} \sum_{t=T_w}^{T-1} \eta_t &= \sum_{t=T_w}^{T-1} \left(\eta_{\min} + (\eta_{\max} - \eta_{\min}) \left(1 - \frac{t - T_w}{T - T_w} \right)^p \right) \geq \eta_{\min} (T - T_w) + (\eta_{\max} - \eta_{\min}) \frac{T - T_w}{p + 1} \\ &= \frac{\eta_{\max} + p \eta_{\min}}{p + 1} (T - T_w) \end{aligned}$$

and

$$\begin{aligned} \sum_{t=T_w}^{T-1} \frac{\eta_t^2}{b_t} &= \sum_{t=T_w}^{T-1} \frac{1}{b_t} \left(\eta_{\min}^2 + (\eta_{\max} - \eta_{\min})^2 \left(1 - \frac{t - T_w}{T - T_w} \right)^{2p} + 2\eta_{\min}(\eta_{\max} - \eta_{\min}) \left(1 - \frac{t - T_w}{T - T_w} \right)^p \right) \\ &\leq \sum_{t=T_w}^{T-1} \frac{\eta_{\max}^2}{b_t} \leq \frac{\eta_{\max}^2 K \zeta(c)}{\underline{a}^{\lfloor c \rfloor}}, \end{aligned}$$

which imply

$$\min_{t \in \{T_w, \dots, T-1\}} \mathbb{E}[\|\text{grad}f(x_t)\|_{x_t}^2] \leq \frac{p + 1}{(2 - L_r \eta_{\max})(\eta_{\max} + p \eta_{\min})} \left(2(f(x_0) - f^*) + \frac{L_r \eta_{\max}^2 K \zeta(c) \sigma^2}{\underline{a}^{\lfloor c \rfloor}} \right) \frac{1}{T - T_w}.$$

□

C.6 Proof of Theorem 4

Proof. **[LR Decay Part: Constant equation 1]**

Considering C.5, we have

$$\sum_{t=T_w}^{T-1} \frac{\eta_t^2}{b_t} = \frac{\eta_{\max}^2}{b} (T - T_w),$$

which implies

$$\min_{t \in \{T_w, \dots, T-1\}} \mathbb{E}[\|\text{grad}f(x_t)\|_{x_t}^2] \leq \frac{2(f(x_0) - f^*)}{(2 - L_r \eta_{\max}) \eta_{\max}} \frac{1}{T - T_w} + \frac{L_r \eta_{\max}}{2 - L_r \eta_{\max}} \frac{\sigma^2}{b}.$$

[LR Decay Part: Diminishing equation 2]

Similarly, we have

$$\sum_{t=T_w}^{T-1} \frac{\eta_t^2}{b_t} = \frac{\eta_{\max}^2}{b} \sum_{t=T_w}^{T-1} \frac{1}{t+1} \leq \frac{\eta_{\max}^2}{b} \left(1 + \int_{T_w}^T \frac{dt}{t}\right) = \frac{\eta_{\max}^2}{b} + \frac{\eta_{\max}^2}{b} \log \frac{T}{T_w},$$

which implies

$$\min_{t \in \{T_w, \dots, T-1\}} \mathbb{E}[\|\text{grad}f(x_t)\|_{x_t}^2] \leq \frac{f(x_0) - f^*}{(2 - L_r \eta_{\max}) \eta_{\max}} \frac{1}{\sqrt{T+1} - \sqrt{T_w+1}} + \frac{L_r \eta_{\max}}{2(2 - L_r \eta_{\max})} \frac{\sigma^2}{b} \frac{1 + \log \frac{T}{T_w}}{\sqrt{T+1} - \sqrt{T_w+1}}.$$

[LR Decay Part: Cosine Annealing equation 3]

Doing the same with C.5, we have

$$\begin{aligned} \sum_{t=T_w}^{T-1} \frac{\eta_t^2}{b_t} &= \frac{1}{b} \sum_{t=T_w}^{T-1} \left(\frac{(\eta_{\max} + \eta_{\min})^2}{4} + \frac{\eta_{\max}^2 - \eta_{\min}^2}{2} \cos \frac{t - T_w}{T - T_w} \pi + \frac{(\eta_{\max} - \eta_{\min})^2}{4} \cos^2 \frac{t - T_w}{T - T_w} \pi \right) \\ &\leq \frac{1}{b} \sum_{t=T_w}^{T-1} \left(\frac{(\eta_{\max} + \eta_{\min})^2}{4} + \frac{\eta_{\max}^2 - \eta_{\min}^2}{2} + \frac{(\eta_{\max} - \eta_{\min})^2}{4} \right) = \frac{\eta_{\max}^2}{b} (T - T_w), \end{aligned}$$

which implies

$$\min_{t \in \{T_w, \dots, T-1\}} \mathbb{E}[\|\text{grad}f(x_t)\|_{x_t}^2] \leq \frac{4(f(x_0) - f^*)}{(2 - L_r \eta_{\max})(\eta_{\max} + \eta_{\min})} \frac{1}{T - T_w} + \frac{2L_r \eta_{\max}^2}{(2 - L_r \eta_{\max})(\eta_{\max} + \eta_{\min})} \frac{\sigma^2}{b}.$$

[LR Decay Part: Polynomial Decay equation 4]

Similarly, we have

$$\begin{aligned} \sum_{t=T_w}^{T-1} \frac{\eta_t^2}{b_t} &= \frac{1}{b} \sum_{t=T_w}^{T-1} \left(\eta_{\min}^2 + (\eta_{\max}^2 - \eta_{\min}^2) \left(1 - \frac{t - T_w}{T - T_w}\right)^{2p} + 2\eta_{\min}(\eta_{\max} - \eta_{\min}) \left(1 - \frac{t - T_w}{T - T_w}\right)^p \right) \\ &\leq \sum_{t=T_w}^{T-1} \frac{\eta_{\max}^2}{b_t} = \frac{\eta_{\max}^2}{b} (T - T_w), \end{aligned}$$

which implies

$$\min_{t \in \{T_w, \dots, T-1\}} \mathbb{E}[\|\text{grad}f(x_t)\|_{x_t}^2] \leq \frac{2(f(x_0) - f^*)(p+1)}{(2 - L_r \eta_{\max})(\eta_{\max} + p\eta_{\min})} \frac{1}{T - T_w} + \frac{2L_r(p+1)\eta_{\max}^2}{(2 - L_r \eta_{\max})(\eta_{\max} + p\eta_{\min})} \frac{\sigma^2}{b}.$$

□

D Objective Function Values in Section 4.1 and Section 4.2

The performance in terms of the objective function value against the number of iterations for LRs equation 1, equation 2, equation 3, and equation 4 on the COIL100, MNIST, MovieLens-1M, and Jester datasets are shown in Figures 7, 8, 9, and 10, respectively.

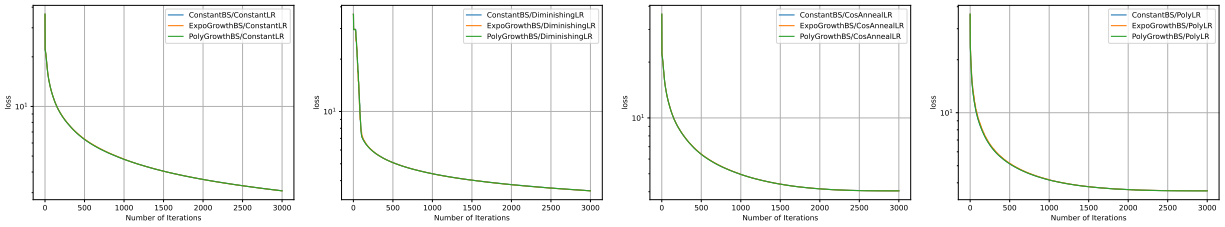


Figure 7: Objective function value against number of iterations for LRs equation 1, equation 2, equation 3, and equation 4 in order from left to right on COIL100 dataset.

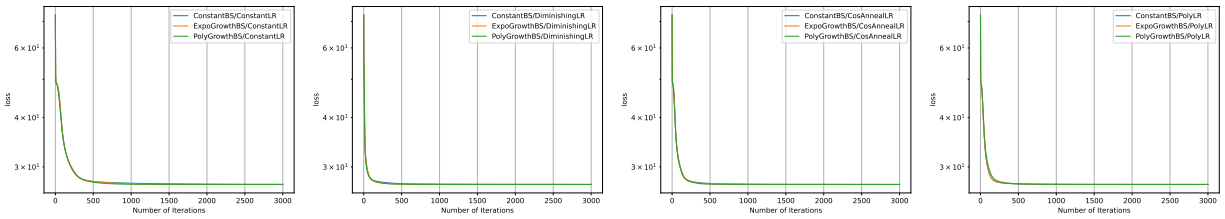


Figure 8: Objective function value against number of iterations for LRs equation 1, equation 2, equation 3, and equation 4 in order from left to right on MNIST dataset.

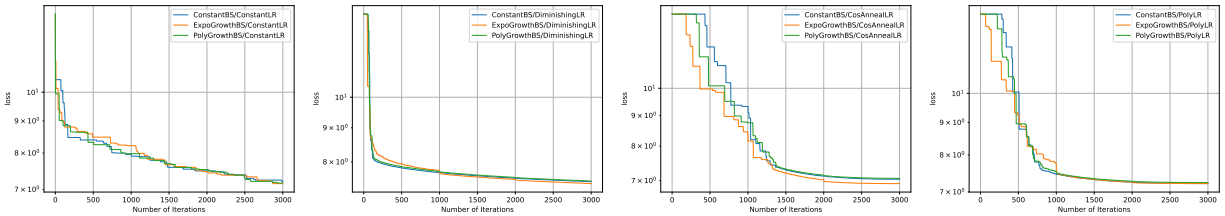


Figure 9: Objective function value against number of iterations for LRs equation 1, equation 2, equation 3, and equation 4 in order from left to right on MovieLens-1M dataset.

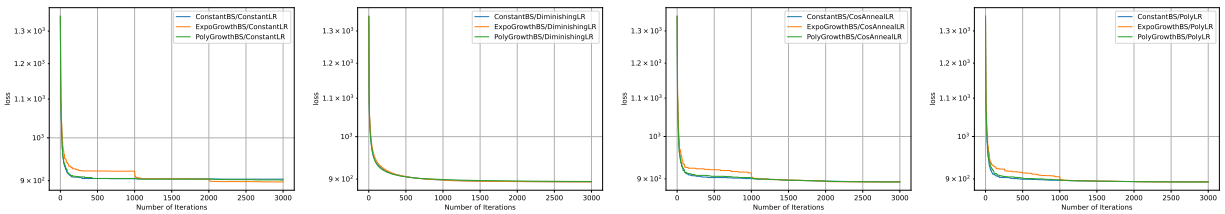


Figure 10: Objective function value against number of iterations for LRs equation 1, equation 2, equation 3, and equation 4 in order from left to right on Jester dataset.

E Additional Numerical Results

This section presents the numerical results for the warm-up LR. We used a constant BS, an exponential growth BS equation 5, a polynomial growth BS equation 6, and a warm-up LR with an increasing part (exponential growth LR) and a decaying part (a constant LR equation 1, a diminishing LR equation 2, a cosine annealing LR equation 3, or a polynomial decay LR equation 4). We set $K' = 200$. When we used an exponential growth LR, a polynomial growth BS was not required to satisfy $\delta^{2l} < \gamma$, but an exponential growth BS was required to satisfy it (see Section 3.3). For comparison, even when using a polynomial growth BS, we used a setting that satisfies this condition. Furthermore, we chose η_{\max} (initial value of decaying part) from $\{0.5, 0.05, 0.005\}$. When using an exponential BS, we set initial batch size $b_0 := 3^4$ in **Cases A, B** and $b_0 := 3^3$ in **Cases C, D**. When using the other BSs, we set the same initial batch size with Section 4. From the definition of exponential growth LR equation 7, we can represent the part after warm-up as $\eta_{T_w-1} = \eta_0 \delta^{l_w}$. Consequently, we chose hyperparameters $(l, l_w, \gamma, \eta_{\max}, \eta_0)$ satisfying $\eta_0 \delta^{l_w} = \eta_{\max}$ and $\delta^{2l} < \gamma$; i.e., $\delta = (\frac{\eta_{\max}}{\eta_0})^{\frac{1}{l_w}} < \gamma^{\frac{1}{2l}}$. Hence, when $l = l_w = 3$ and $\gamma = 3.0$, we set $\eta_{\max} = 0.5, 0.05, 0.005$ and $\eta_0 = \frac{5}{17}, \frac{5}{170}, \frac{5}{1700}$ respectively. In this setting, $\delta = \sqrt[3]{\frac{\eta_{\max}}{\eta_0}} = \sqrt[3]{1.7} < \sqrt[6]{3} = \sqrt[6]{\gamma} = \gamma^{\frac{1}{2l}}$ holds. And, when $l = 3, l_w = 8, \gamma = 3$, we set $\eta_{\max} = 0.5, 0.05, 0.005$, $\eta_0 = \frac{1}{8}, \frac{1}{80}, \frac{1}{800}$ respectively. In this setting, $\delta = \sqrt[8]{\frac{\eta_{\max}}{\eta_0}} = \sqrt[8]{4} < \sqrt[6]{3} = \sqrt[6]{\gamma} = \gamma^{\frac{1}{2l}}$ holds. Since we terminated RSGD after the 3000th iteration and set $K' = 200$, $l = l_w = 3$ (resp. $l = 3, l_w = 8$). Those settings mean 5 times BS increasing and 3 times LR increasing (resp. 5 times BS increasing and 8 times LR increasing).

E.1 Principle Components Analysis

[Case A] $l = l_w = 3$

Figures 11 and 13 plot performance in terms of the gradient norm of the objective function against the number of iterations for a warm-up LR with decay parts equation 1, equation 2, equation 3, and equation 4 on the COIL100 and MNIST datasets, respectively. Figures 12 and 14 plot performance in terms of the objective function value against the number of iterations for a warm-up LR with decay parts equation 1, equation 2, equation 3, and equation 4 for the COIL100 and MNIST datasets, respectively.

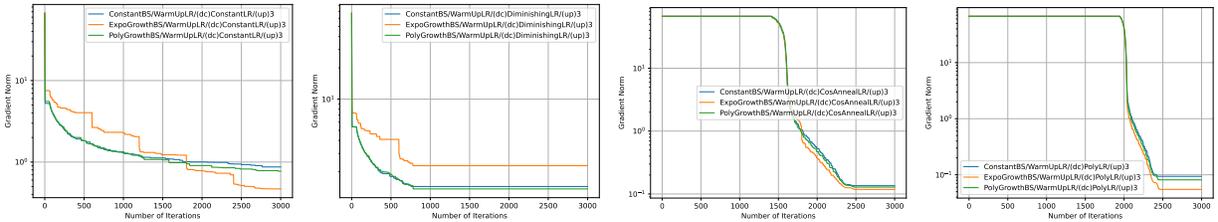


Figure 11: Norm of the gradient of the objective function against number of iterations for warm-up LR that have an increasing part with three increments on COIL100 dataset.

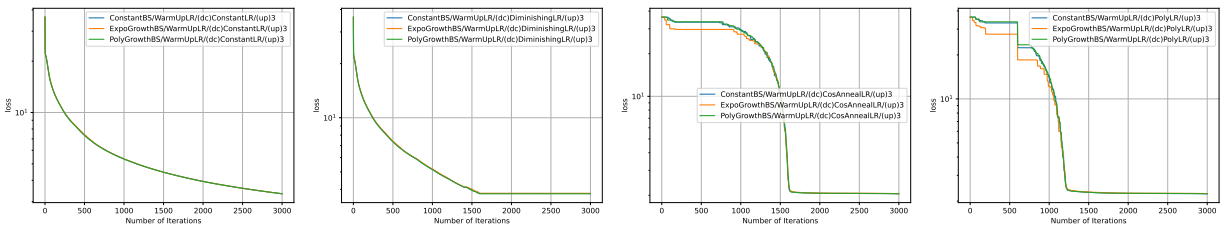


Figure 12: Objective function value against number of iterations for warm-up LR that have an increasing part with three increments on COIL100 dataset.

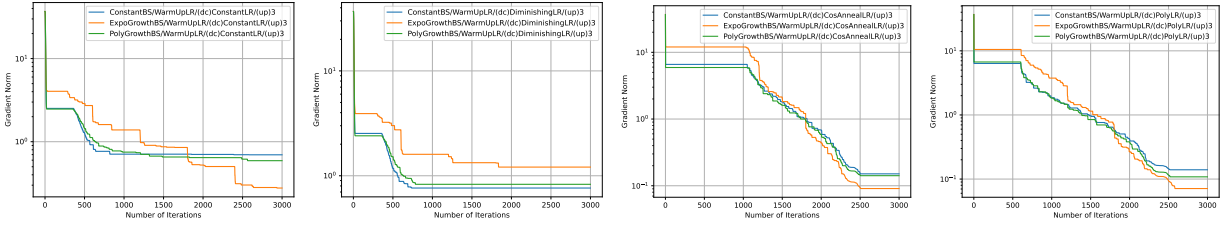


Figure 13: Norm of the gradient of the objective function against number of iterations for warm-up LR schedules that have an increasing part with three increments on MNIST dataset.

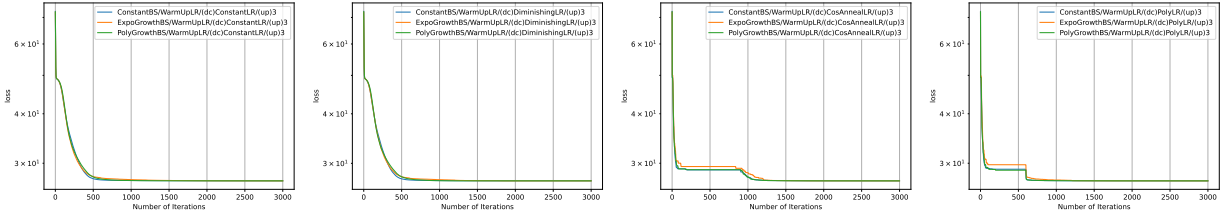


Figure 14: Objective function value against number of iterations for warm-up LR schedules that have an increasing part with three increments on MNIST dataset.

[Case B] $l = 3, l_w = 8$

Figures 15 and 17 plot the performance in terms of the gradient norm of the objective function against the number of iterations for a warm-up LR with decay parts equation 1, equation 2, equation 3, and equation 4 for the COIL100 and MNIST datasets, respectively. Figures 16 and 18 plot the performance in terms of the objective function value against the number of iterations of a warm-up LR with decay parts equation 1, equation 2, equation 3, and equation 4 for the COIL100 and MNIST datasets, respectively.

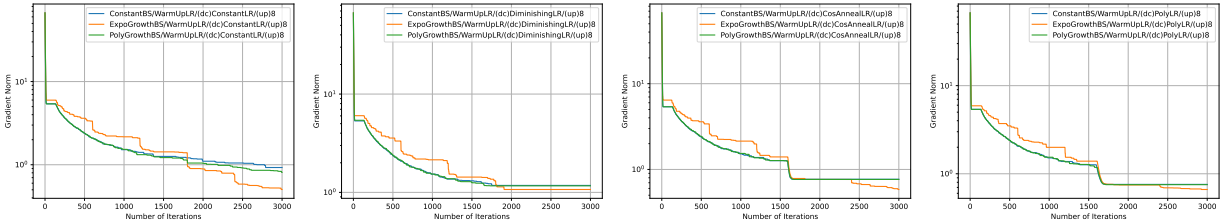


Figure 15: Norm of the gradient of the objective function against number of iterations for warm-up LR schedules that have an increasing part with eight increments on COIL100 dataset.

E.2 Low-rank Matrix Completion

[Case C] $l = l_w = 3$

Figures 19 and 21 plot the performance in terms of the gradient norm of the objective function against the number of iterations for a warm-up LR with decay parts equation 1, equation 2, equation 3, and equation 4 on the MovieLens-1M and Jester datasets, respectively. Figures 19 and 22 plot the performance in terms of the objective function value against the number of iterations for a warm-up LR with decay parts equation 1, equation 2, equation 3, and equation 4 on the MovieLens-1M and Jester datasets, respectively.

[Case D] $l = 3, l_w = 8$

Figures 23 and 25 plot the performance in terms of the gradient norm of the objective function against the number of iterations for a warm-up LR with decay parts equation 1, equation 2, equation 3, and equation 4 on the MovieLens-1M and Jester datasets, respectively. Figures 23 and 26 plot the performance in terms of

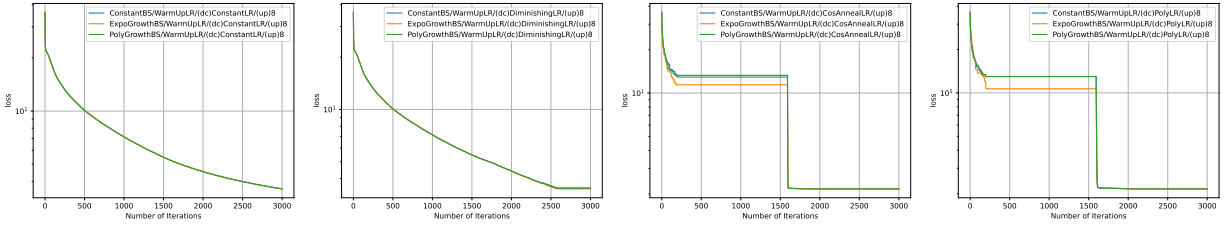


Figure 16: Objective function value against number of iterations for warm-up LR that have an increasing part with eight increments on COIL100 dataset.

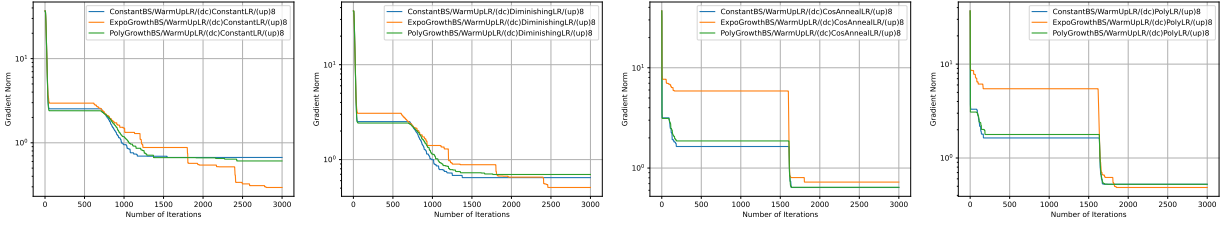


Figure 17: Norm of the gradient of the objective function against number of iterations for warm-up LR that have an increasing part with eight increments on MNIST dataset.

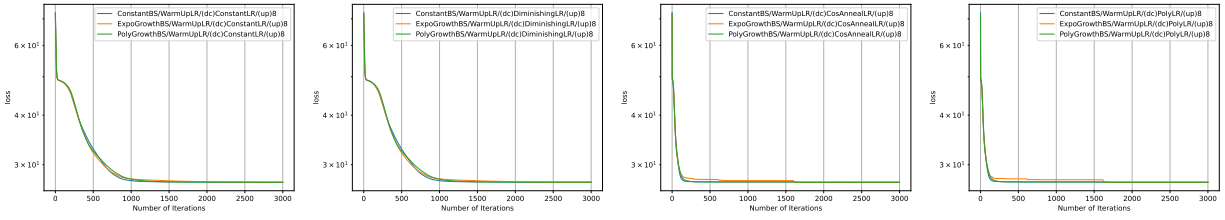


Figure 18: Objective function value against number of iterations for warm-up LR that have an increasing part with eight increments on MNIST dataset.

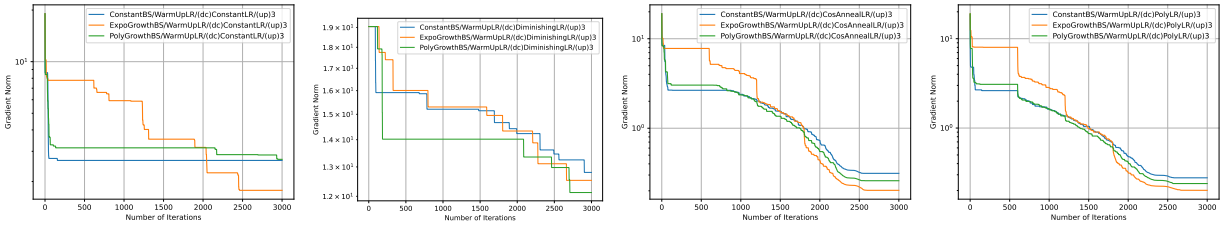


Figure 19: Norm of the gradient of the objective function against number of iterations for warm-up LR that have an increasing part with three increments on MovieLens-1M dataset.

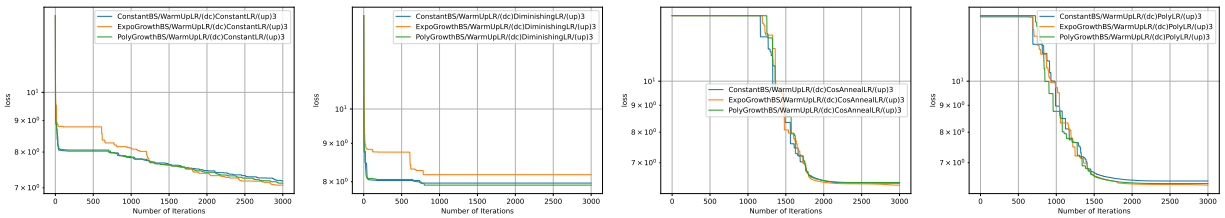


Figure 20: Objective function value against number of iterations for warm-up LR that have an increasing part with three increments on MovieLens-1M dataset.

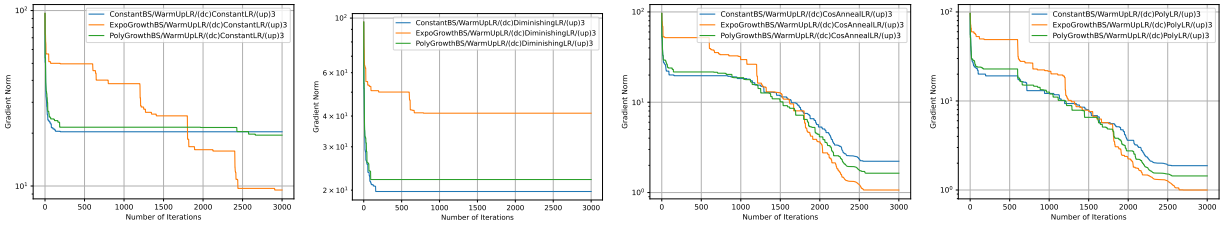


Figure 21: Norm of the gradient of the objective function against number of iterations for warm-up LR that have an increasing part with three increments on Jester dataset.

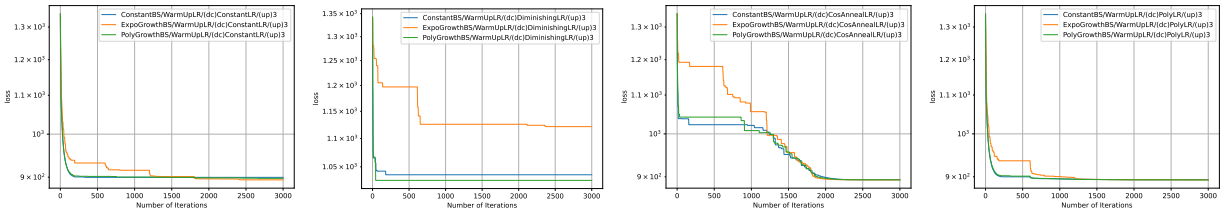


Figure 22: Objective function value against number of iterations for warm-up LR that have an increasing part with three increments on Jester dataset.

the objective function value against the number of iterations for a warm-up LR with decay parts equation 1, equation 2, equation 3, and equation 4 on the MovieLens-1M and Jester datasets, respectively.

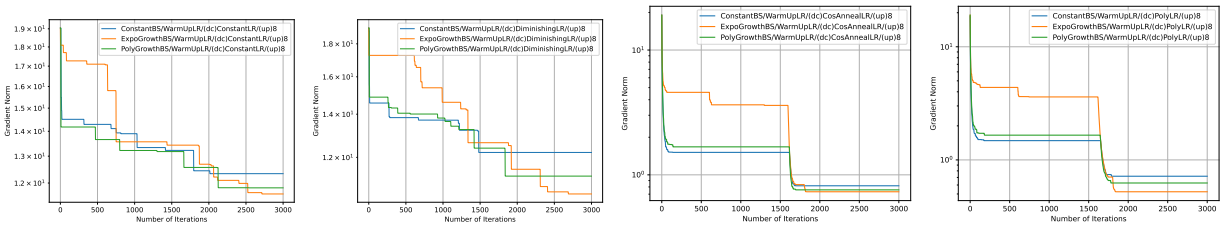


Figure 23: Norm of the gradient of the objective function against number of iterations for warm-up LR that have an increasing part with eight increments on MovieLens-1M dataset.

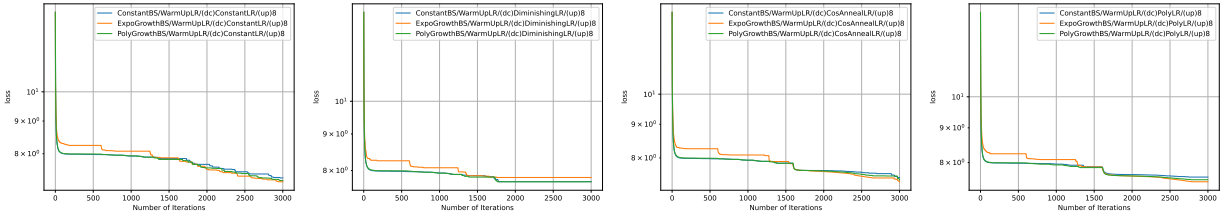


Figure 24: Objective function value against number of iterations for warm-up LR that have an increasing part with eight increments on MovieLens-1M dataset.

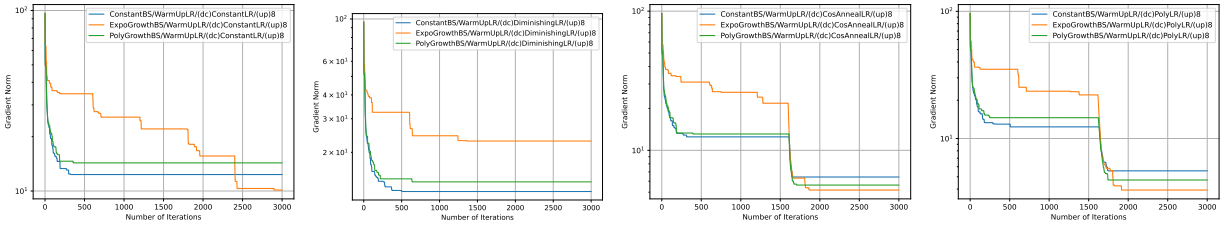


Figure 25: Norm of the gradient of the objective function against number of iterations for warm-up LR that have an increasing part with eight increments on Jester dataset.

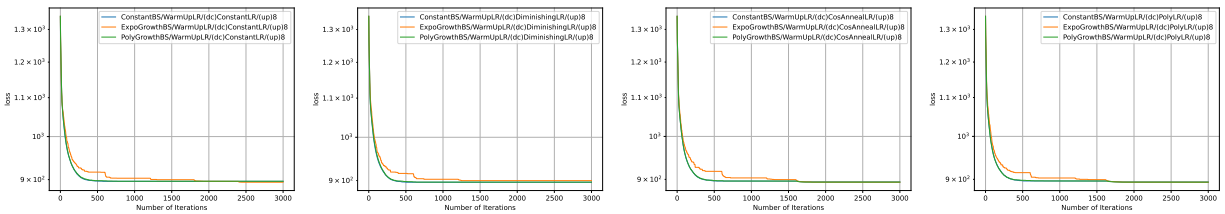


Figure 26: Objective function value against number of iterations for warm-up LR that have an increasing part with eight increments on Jester dataset.